AD-A110 318 FOREIGN TECHNOLOGY DIV WRIGHT-PATTERSON AFB OH F/G 9/5
ANTENNY (SELECTED ARTICLES),(U)
JAN 82 S M VEREVKIN, I P IVANOV
UNCLASSIFIED FTD-ID(RS)T-1091-81 NL

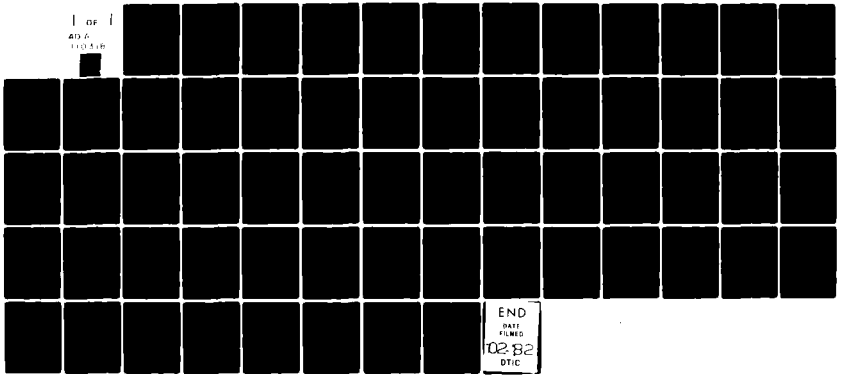

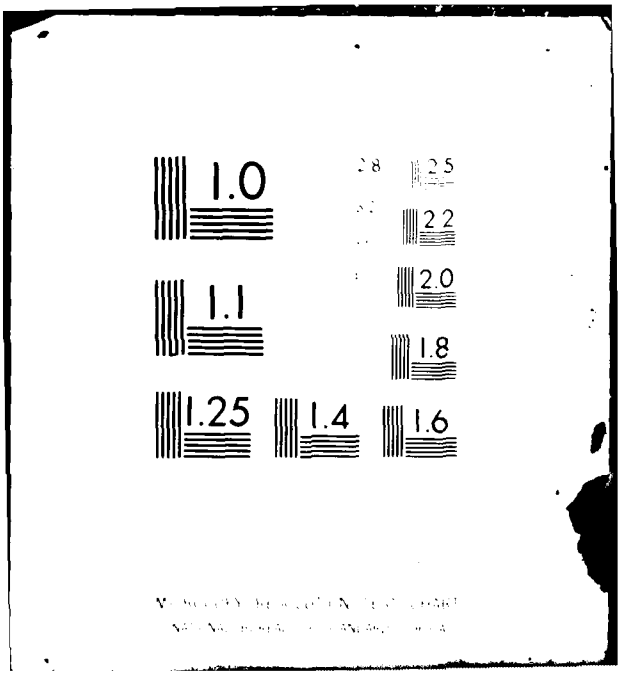
1.0
1.1
1.25
1.4
1.6
1.8
2.0
2.2
2.5

FTD-ID(RS)T-1091-81

(2)

FOREIGN TECHNOLOGY DIVISION

ANTENNY

(Selected Articles)

Approved for public release;
distribution unlimited.

DISCLAIMER NOTICE

THIS DOCUMENT IS BEST QUALITY PRACTICABLE. THE COPY FURNISHED TO DTIC CONTAINED A SIGNIFICANT NUMBER OF PAGES WHICH DO NOT REPRODUCE LEGIBLY.

EDITED TRANSLATION

FTD-ID(RS)T-1091-81 14 January 1982

MICROFICHE NR: FTD-82-C-000024

ANTENNY (Selected Articles)

English pages: 56

Source: Antenny, Nr. 5, 1969, pp. 61-107

Country of origin: USSR
Translated by: SCITRAN
F33657-81-D-0263
Requester: USAMICOM

PREPARED BY:

TRANSLATION DIVISION
FOREIGN TECHNOLOGY DIVISION
WP-AFB, OHIO.

Table of Contents

U. S. BOARD ON GEOGRAPHIC NAMES TRANSLITERATION SYSTEM

Block	Italic	Transliteration	Block	Italic	Transliteration
А а	*А а*	A, a	Р р	*Р р*	R, r
Б б	*Б б*	B, b	С с	*С с*	S, s
В в	*В в*	V, v	Т т	*Т т*	T, t
Г г	*Г г*	G, g	У у	*У у*	U, u
Д д	*Д д*	D, d	Ф ф	*Ф ф*	F, f
Е е	*Е е*	Ye, ye; E, e*	Х х	*Х х*	Kh, kh
Ж ж	*Ж ж*	Zh, zh	Ц ц	*Ц ц*	Ts, ts
З з	*З з*	Z, z	Ч ч	*Ч ч*	Ch, ch
И и	*И и*	I, i	Ш ш	*Ш ш*	Sh, sh
Й й	*Й й*	Y, y	Щ щ	*Щ щ*	Shch, shch
К к	*К к*	K, k	Ъ ъ	*Ъ ъ*	"
Л л	*Л л*	L, l	Ы ы	*Ы ы*	Y, y
М м	*М м*	M, m	Ь ь	*Ь ь*	'
Н н	*Н н*	N, n	Э э	*Э э*	E, e
О о	*О о*	O, o	Ю ю	*Ю ю*	Yu, yu
П п	*П п*	P, p	Я я	*Я я*	Ya, ya

*ye initially, after vowels, and after ъ, ь; e elsewhere.
When written as ё in Russian, transliterate as yё or ё.

RUSSIAN AND ENGLISH TRIGONOMETRIC FUNCTIONS

Russian	English	Russian	English	Russian	English
sin	sin	sh	sinh	arc sh	sinh^{-1}
cos	cos	ch	cosh	arc ch	cosh^{-1}
tg	tan	th	tanh	arc th	tanh^{-1}
ctg	cot	cth	coth	arc cth	coth^{-1}
sec	sec	sch	sech	arc sch	sech^{-1}
cosec	csc	csch	csch	arc csch	csch^{-1}

Russian	English
rot	curl
lg	log

OPTIMIZATION OF THE MAIN RADIO ENGINEERING CHARACTERISTICS OF HIGHLY EFFICIENT LOW-NOISE ANTENNAS [6]

S. M. Verevkin, I. P. Ivanov and B. A. Poperechenko

The surface utilization factor and the scattering coefficient of reflecting parabolic antennas has been investigated theoretically and experimentally as a function of the focal distance of the mirror and of the radiation pattern of the emitter. A number of quantitative data is presented and the optimum values of the parameters, their criticality and the possibility of practical realization are evaluated.

The radio engineering characteristics of highly efficient low-noise parabolic antennas can be optimized mainly by selecting the ratio f/D, the shape of the radiation pattern of the main mirror, the radiation diagram and design of the emitter. It is these factors that primarily determine the most efficient field distribution at the aperture and the minimum scattering coefficient of the antenna with optimum shape of the radiation pattern.

No adequate quantitative data can be found in the known numerous literature that permits the indicated optimization. Published results are related mainly to antennas with main mirror radiation pattern of type $\cos^n\varphi$. As is shown below, these patterns are rather far from the optimum shape.

The maximum result in the ratio of the surface utilization factor (kip) of a parabolic antenna and the energy scattering coefficient of the emitter β are

provided by radiation patterns of special shape closer to ideal patterns given in Figure 1: 1—at $2\psi_0 = 120°$ and 2—at $2\psi_0 = 220°$. However, it is understandable that infinite curvature of the slope of the radiation pattern cannot be realized. The degree of approximation to ideal patterns is determined by the design characteristics of the emitter and the radiation diagram.

Theoretical and experimental investigation was conducted with respect to a double-reflector radiation diagram of the main mirror.

The calculation and theoretical part of the investigation utilizes the results of finding the surface utilization factor and the radiation scattering coefficient with regard to the most important factors: the antenna configuration and emitter characteristics. The aperture angle of the main antenna mirror is taken in the range of $2\psi_0 = 120°$–$220°$ (f/D = 0.435–0.175). Analytical representation of the radiation pattern of special shape is taken in the form:

$$\text{for the range} \quad 0 \leq \psi \leq \gamma \quad \frac{F(\psi)}{F(0)} = \frac{1}{\cos^2 \frac{\gamma}{2}} \left[A + (1-A) \left(\frac{\psi}{\gamma} \right)^2 \right], \tag{1}$$

$$\text{for the range} \quad \gamma \leq \psi \leq \psi_m \quad \frac{F(\psi)}{F(0)} = \frac{1}{\cos^2 \frac{\gamma}{2}} \cos \left[\arccos \tau \left(\frac{\psi - \gamma}{\psi_0 - \gamma} \right) \right], \tag{2}$$

$$\text{for the range} \quad \psi_m \leq \psi \leq \pi \quad \frac{F(\psi)}{F(0)} = -0{,}15 \cos \left(\frac{\pi}{2} \frac{\pi - \psi}{\psi_m} \right). \tag{3}$$

The shape of this radiation pattern is shown by curve 3 in Figure 1. Angles ψ_0 and ψ_m and levels A and τ are shown in the same figure.

The analytical representation is far from the only one and cannot claim complete detailed similarity to real radiation patterns of special shape. Nevertheless this representation retains all the principal characteristics of the radiation patterns of interest and permits one to determine all the most important principles for quantitative estimates.

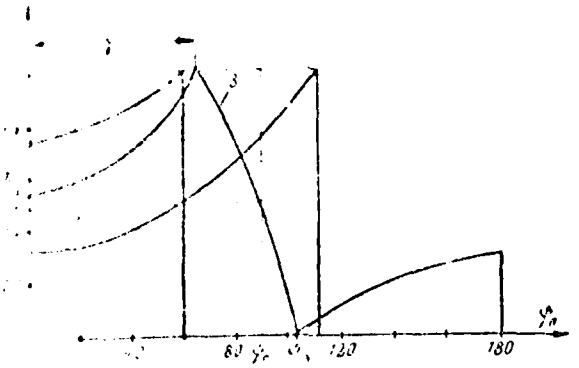

Figure 1.

... utilization factor (K) and the scattering coefficient β were calculated from formulas:

$$K = \frac{2\operatorname{ctg}^2\frac{\psi_0}{2}\left[\int_0^{\psi_0}\frac{E(\psi)}{E(0)}\operatorname{tg}\frac{\psi}{2}d\psi\right]}{\int_0^{\pi}\left[\frac{E(\psi)}{E(0)}\right]^2\sin\psi\,d\psi}, \qquad (4)$$

$$\beta = \frac{\int_{\psi_0}^{\pi}\left[\frac{E(\psi)}{E(0)}\right]^2\sin\psi\,d\psi}{\int_0^{\pi}\left[\frac{E(\psi)}{E(0)}\right]^2\sin\psi\,d\psi}. \qquad (5)$$

03

... results of calculating K and β in the range of parameters are presented ... 2, 3, 4 and 5. One can make quite specific conclusions on the basis of ..., which are confirmed experimentally below.

... can be seen from the indicated series of graphs, the highest value of the ... utilization factor is reached for antennas with aperture of $2\psi_0 \approx 180°$ at ... angle of the maximum radiation pattern $2\gamma = 2\psi_0 - 20°$. For a ... of 2γ, there is a tendency toward a shift of the maximum value

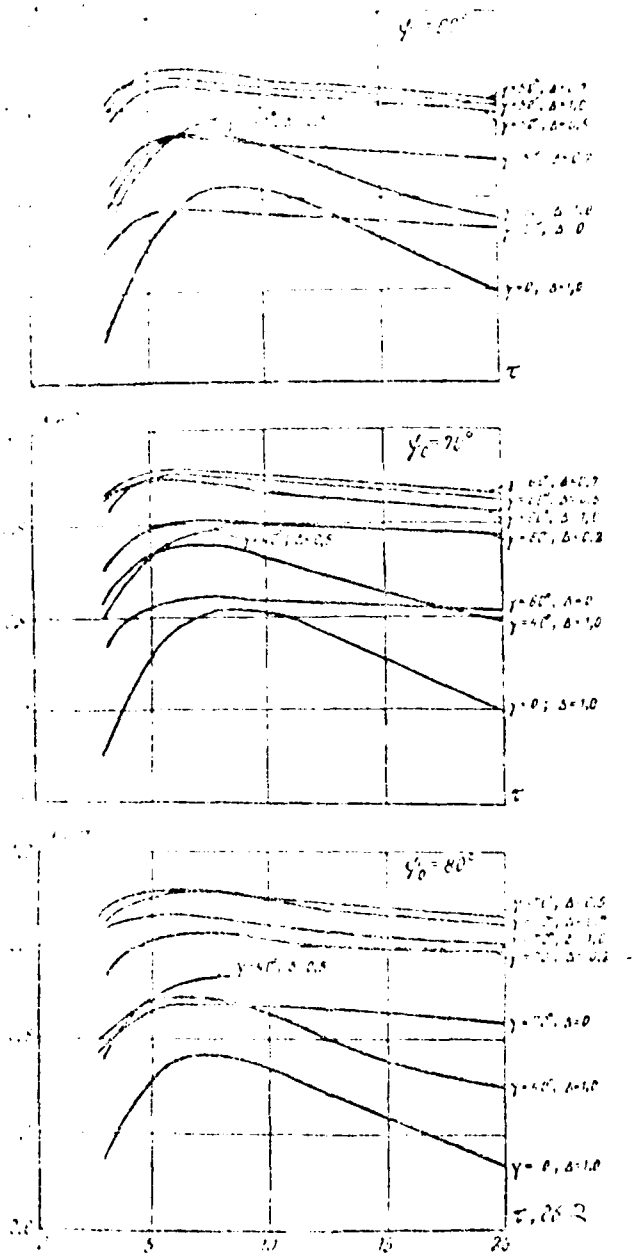

Figure 2.

...e calibration factor 2— dB

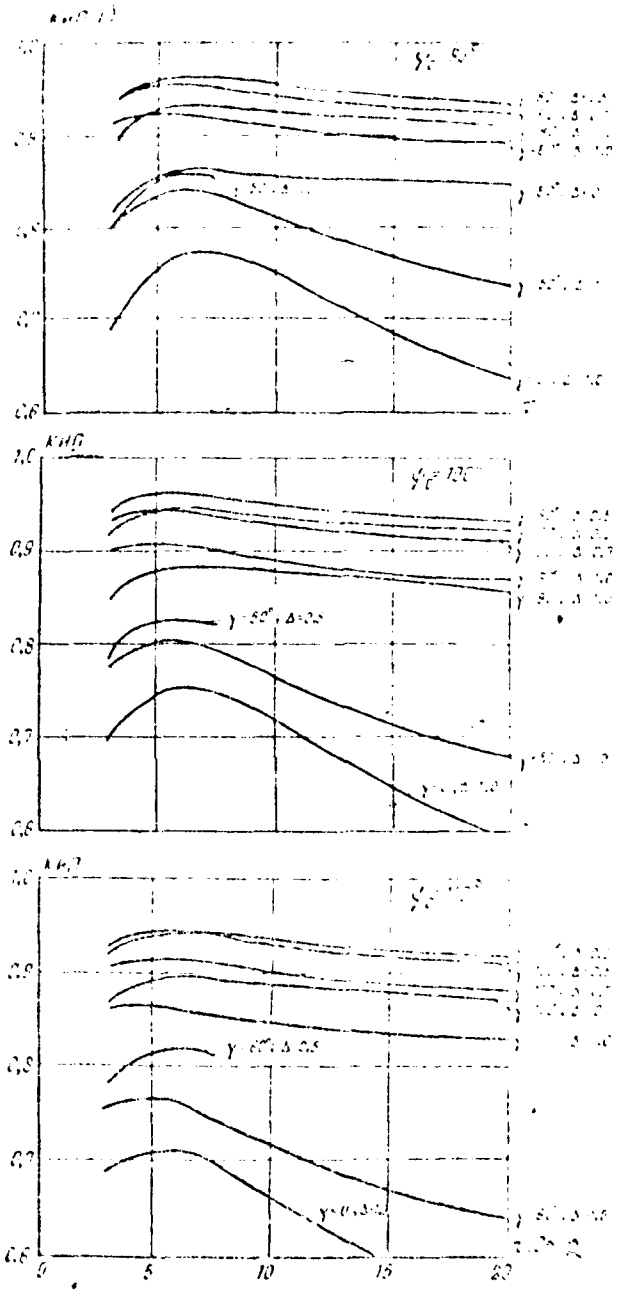

Figure 3.

- (Face utilization factor 2— 65

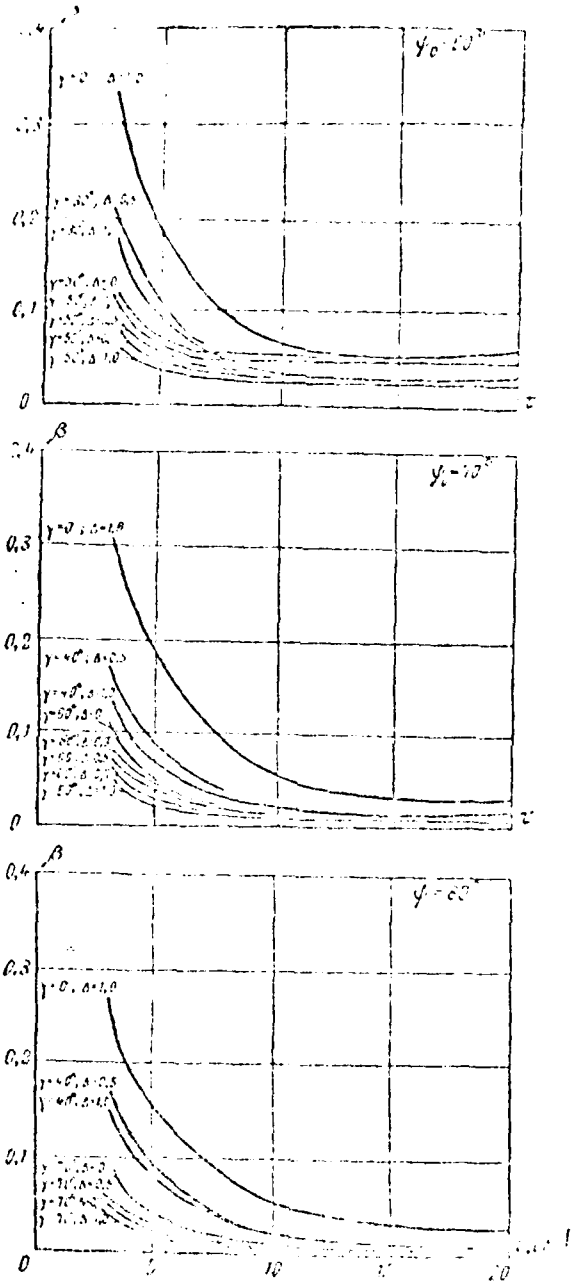

Figure 4.

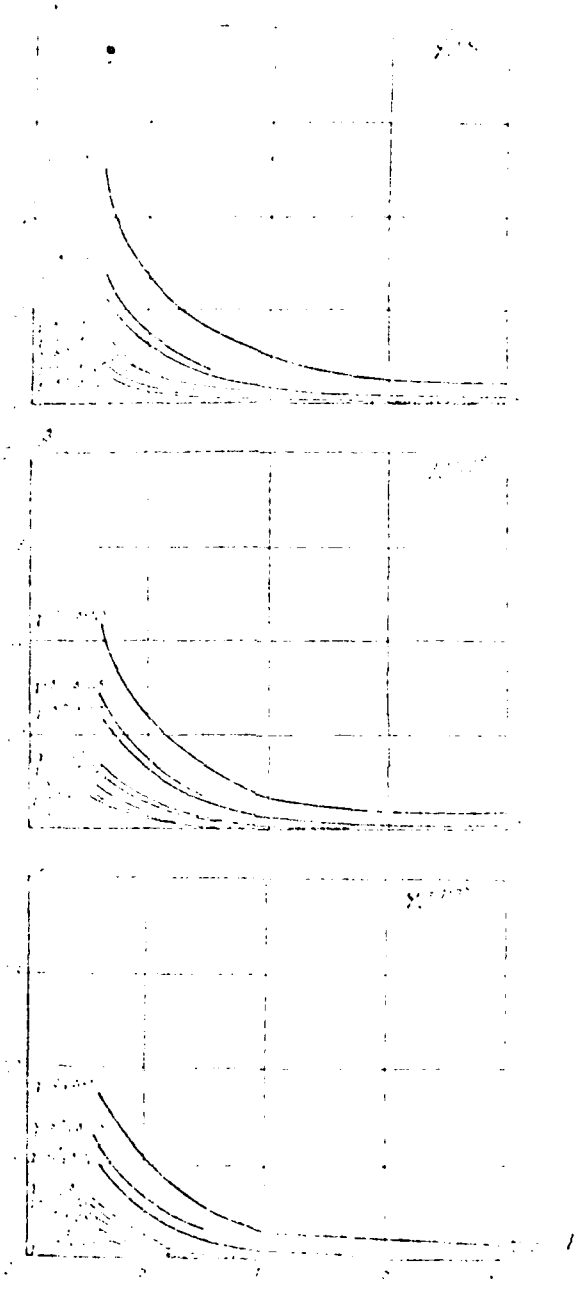

Figure 5.

of the surface utilization factor toward smaller aperture angles $2\psi_0$. Thus, for $2\gamma = 2\psi_0 - (60\text{-}80)$, the maximum surface utilization factor occurs at $2\psi_0 \approx 140°$, while the maximum surface utilization factor corresponds to $2\psi_0 < 120°$ for $2\gamma = 0$.

This circumstance is easy to explain if one bears in mind that the minimum distance from the emitter to the edge of the mirror occurs at f/D = 0.25 with given antenna diameter. In this case the peripheral zone of the aperture near the edges of the mirror, corresponding to the region of slope in the radiation pattern of special shape, has the least area. The peripheral zone of the aperture increases upon deviation of f/D from the indicated extreme value since the angular dimension of the region of the slope is fixed and the distance to the edge of the mirror increases.

A decrease of the extreme value of $2\psi_0$ as the beam angle of the maximum radiation pattern 2γ decreases should be related to the fact that the contribution of the peripheral zone of the aperture to the surface utilization factor increases at lower values of 2γ, where the field distribution is considerably nonuniform. Therefore, the highest surface utilization factor is provided in these cases in longer-focus antennas where an increase of focal distance partially compensates for this nonuniformity.

Thus, optimum selection of the aperture angle of the antenna mirror $2\psi_0$ is dependent on the possibility of realizing the corresponding steepness of the slope of the radiation pattern. The use of emitters with special shape of the radiation pattern with angle $2\gamma = 2\psi_0 - 20°$ permits one to increase the surface utilization factor in the range of angles $2\psi_0 = 120\text{-}220$ compared to a pattern of cos^3 for 0.12-0.22°, respectively. In this case the highest calculated surface utilization factor corresponds 0.96 for $2\psi_0 = 180°$.

Let us now turn to the dependence of the surface utilization factor on the level of illumination of the edge of the mirror τ. One should note in this regard the very weak dependence of the surface utilization factor $\sigma\tau$ for radiation patterns with the greatest beam angle 2γ (2-3 percent in the range of $\tau = -(7\text{-}15)$ dB) regardless of f/D. The criticality of the value of τ increases as 2γ decreases

and is highest for radiation patterns of type $\cos^{q}\psi$ ($2\gamma = 0$). In this case the optimum value of τ increases from -(5-6) dB at $2\gamma = 2\psi_0 - 20°$ to -(7-9) dB at $2\gamma = 0$. 68

Thus, selecting the optimum radiation of the edge of the mirror is essentially undetermined by the requirements with respect to the surface utilization factor. As will be seen from what follows, optimization of the level of radiation of the edge of the mirror is determined primarily by the requirements on the scattering coefficient.

Finally, let us estimate the effect of the depth of the valley in the radiation pattern Δ. As follows from the graphs of the surface utilization factor, the optimum value of Δ corresponds to approximately uniform aperture distribution in the zone $\pm\gamma$ and is equal to $\Delta = \cos^{2(q+1)}\gamma$. Deviation of Δ from this value by 0.1-0.2 for $2\gamma = 2\psi_0 = 20°$ has no significant effect on the surface utilization factor. The permissible range of variation of Δ expands somewhat as 2γ decreases.

Let us turn to consideration of the scattering coefficient β (see Figures 4 and 5). The first thing that attracts attention in the indicated graphs is the appreciably higher value of β for radiation patterns of type $\cos^{q}\psi$ compared to those of special shape, especially when compared to patterns with angle $2\gamma = 2\psi_0 - 20°$.

It is also typical that the scattering coefficient β decreases independently of the nature of the radiation pattern as the beam angle of the mirror $2\psi_0$ increases. Finally, yet another characteristic feature should be noted which includes the fact that, beginning at some level of radiation of the mirror edge τ, the scattering coefficient essentially does not decrease with a further decrease of it since it is determined in this case of τ by the relative level of the back radiation of the emitter.

This "threshold" value of τ is different for different types of radiation patterns. Thus, this value is $\tau = -(10-12)$ dB for a pattern of type $\cos^{q}\psi$, $\tau = -(7-9)$ dB for a pattern of special shape with angle $2\gamma = 2\psi_0 - (60-80)$ and $\tau = -5$ dB for a pattern with angle $2\gamma = 2\psi_0 - 20°$.

This difference in the relative level of the field in the direction of the edge of the mirror τ for different radiation patterns is determined by the fact that the scattering capacity in the range of part of the main lobe of the pattern outside sector $2\psi_0$ is significantly dependent on the steepness of its slope. Thus, if the steepness of the slope is high this part of the capacity decreases significantly and the possibility of softening of the requirements appears with regard to the level of radiation of the mirror edge τ.

Moreover, the surface utilization factor of the emitter decreases somewhat for special radiation patterns. As a result it also becomes possible to increase the relative level of field τ while retaining the same surface utilization factor in the direction of the mirror edge and the previous value of the scattering coefficient.

By comparing the effect of the shape of the radiation pattern, the radiation level of the edge of the main mirror τ and its aperture angle $2\psi_0$ on the reduction of scattering coefficient β, one can definitely say that selecting the type of radiation pattern and radiation level of the mirror edge and finally the level of back radiation of the emitter is the most significant in this regard. The aperture angle $2\psi_0$ has a much less significant effect on the scattering coefficient. 69

Use of radiation patterns of special shape permits one to reduce the scattering coefficient by not less than a factor of two compared to patterns of type $\cos\psi$.

Since selection of the radiation level of the mirror edge has little effect on the surface utilization factor over a rather wide range, the optimum value of τ is mainly determined by the requirements in the ratio of the scattering coefficient. A value of $\tau = -(6\text{-}8)$ dB can be recommended for radiation patterns of special shape. In this case the scattering coefficient will comprise an average of approximately 3-5 percent. However, it should be stipulated here that this value is determined chiefly by the power emitted by the emitter to the back hemisphere.

The value of β varies proportionally upon variation of this power compared to the value of -(16-17) dB used in the given calculations.

With regard to optimum selection of the aperture angle $2\psi_0$, then as can be seen from the graphs in Figures 2-5, the effect of $2\psi_0$ on the surface utilization factor and β is not very critical.

Therefore, $2\psi_0$ can be selected individually in each specific case depending on the requirements on the surface utilization factor and β. Nevertheless the feasibility of increasing $2\psi_0$ above 120° is obvious since this leads to some reduction of the surface utilization factor, essentially does not reduce β and causes additional design complications in the mirror, support-rotational device and antenna drives.

The results of calculating the variation of the surface utilization factor and β as a function of angle $2\psi_0$ are presented below for several experimental patterns of special shape. Different logospiral conical emitters were used in this case. Selection in favor of these emitters was determined by their advantages over other types of antennas. These emitters permit one to maintain the axial symmetry of the radiation patterns for both components of the field vector and satisfactory polarization characteristics over a wide range of frequencies and shapes of the radiation pattern.

The required shape of the pattern is determined by selection of the angle at the vertex of the cone and the angle of elevation of the spiral. The pattern is additionally obtained by defining the number of turns and the dimensions and shape of the reflector.

A series of experimental radiation patterns of logospiral emitters is presented in Figure 6. The calculated values of the aperture surface utilization factor, the total surface utilization factor and the scattering coefficient β are presented in Table 1 for these same patterns. These three values are related to each other by the following known relation: 70

$$K = K_a(1 - \beta). \tag{6}$$

... surface utilization factor, K_a is the aperture surface util... the scattering coefficient of the emitter.

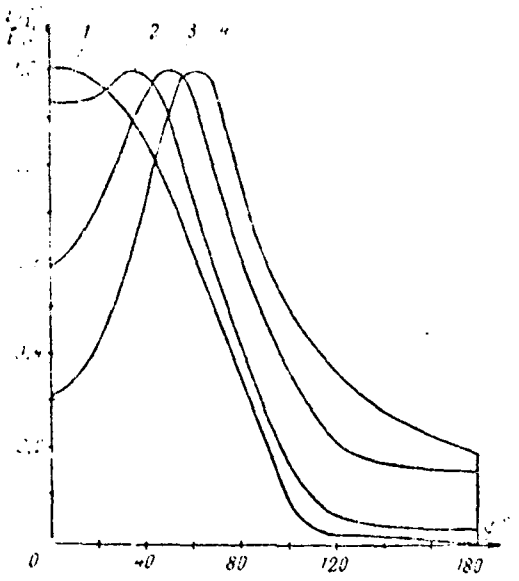

Figure 6.

The total surface utilization factor and scattering coefficient β are determined from expressions (4) and (5) by numerical integration of the given experimental radiation patterns.

The aperture surface utilization factor can be calculated by the formula

$$K_a = \frac{2\operatorname{ctg}^2\frac{\psi_0}{2}\left[\int_0^{\psi_0}\frac{F(\psi)}{F(0)}\operatorname{tg}\frac{\psi}{2}\,d\psi\right]^2}{\int_0^{\pi}\left[\frac{F(\psi)}{F(0)}\right]^2\sin\psi\,d\psi} \tag{7}$$

or can be found from expression (6) with known values of K and β. The surface utilization factor was measured on a model of a parabolic antenna for an emitter with radiation pattern 3 (Figure 6) by the method of comparison to a reference horn antenna.

Moreover, the values of the total surface utilization factor were measured by the radio astronomy method [1] on 20 aerial antennas of the Orbita stations, where an emitter with this pattern is installed. A value of the surface utilization factor equal to an average of 0.73 was found in both cases, which is in good agreement with the given data in Table 1. 71

Table 1

Variants	Parameters	$2\psi_0$ 120°	140°	160°	180°
Radiation pattern 1	Aperture kip *	0.96	0.88	0.84	0.73
	β	0.24	0.13	0.06	0.02
	k_{sp}	0.73	0.77	0.79	0.71
Radiation pattern 2	Aperture kip	0.97	0.91	0.86	0.76
	β	0.29	0.17	0.09	0.04
	kip	0.68	0.75	0.78	0.73
Radiation pattern 3	Aperture kip	0.98	0.96	0.94	0.85
	β	0.43	0.27	0.15	0.08
	kip	0.56	0.7	0.8	0.78
Radiation pattern 4	Aperture kip	0.94	0.94	0.96	0.91
	β	0.63	0.46	0.3	0.2
	kip	0.35	0.51	0.67	0.73

The given experimental data mainly confirm the principles that follow from the results of calculation. However, one should also note another characteristic feature of experimental patterns related directly to the properties of a specific emitter design. One has in mind here the cross-correlation between the depth of the trough in the axial direction and the level of back radiation. This relationship can be attenuated by increasing the overall dimensions of the emitter and complicating its design and permits one to additionally improve the characteristics, bringing them even closer to the potentially possible characteristics.

Thus, the theoretical and experimental investigations determined the principal engineering solutions that permit one to refine the increased radio emission characteristics of parabolic antennas by relatively simple methods.

Translator's Note: kip = surface utilization factor.

References

1. Богомолов А. Ф., Веревкин [illegible] М., [illegible] Б. А., Козлов Н. Ф. [illegible]

I. V. Vavilova

The geometric utilization factor was investigated in two-mirror antennas of circular symmetry when the aperture of the small mirror that corrects spherical aberration is less than 0.05 of the diameter of the large mirror. A method of calculating the small mirror is presented for a two-mirror system with large mirror in the form of a circular cylinder.

Introduction

Let us call antennas in which the large mirror is a toroidal surface two-mirror of circular symmetry. The profile of the generatrix of the toroid depends on the requirements on the shape of the radiation pattern in the vertical plane and can generally be any profile. The small mirror is calculated so as to correct spherical aberration inherent to a toroidal mirror and to ensure formation of the given pattern. Antennas of circular symmetry permit one to control the beam in a wide sector in one plane only with large mirror fixed by moving the small mirror with emitter along some circumference whose center O_1 is located on axis OO' of the toroid (Figure 1). In the special case when the large mirror is a part of a sphere, the beam can be controlled in space by moving the small mirror with emitter along the surface of a sphere concentric with the large mirror.

The latest systems are known under the name of spherical two-mirror antennas. The large mirror having a form permits large antennas to be developed on the

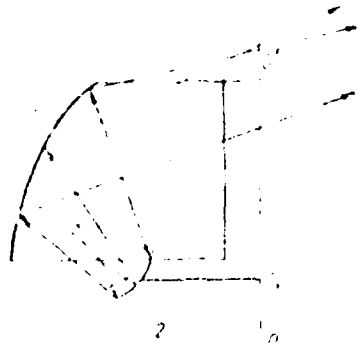

1 large toroidal mirror
2 small correcting mirror
3 primary emitter

Figure 1.

basis. There are now several similar antennas and among them is a five-meter antenna designed to operate in the millimeter band, constructed in Armenia [1].

Another special variant of the two-mirror antenna of circular symmetry, which is of interest to develop large instruments, is an antenna with the large mirror in the form of a circular cylinder 1 (Figure 2).

If a spherical wave source is used as the primary emitter 3, the small mirror in the vertical plane should have a parabolic profile 2. It is more convenient to use an asymmetrical parabola since the receiving apparatus can be located near the emitter and one can avoid shading of the emitting aperture.

This antenna permits one to control the beam only in a single horizontal plane. An additional plane mirror 4 can be used for control in the other plane, i.e., one can operate by the periscope scheme (Figure 2). This version of the antenna is intriguing since it can be realized on the basis of an antenna with variable profile reflector (AFP) [2], which is recommended by Soviet specialists to create giant radio telescopes (for example, the RATAN-600).

The theory and calculation of spherical two-mirror antennas have been developed [3]. It is shown that the existing aperture of a large mirror is considerably dependent on that of the small mirror and their mutual position. However, the

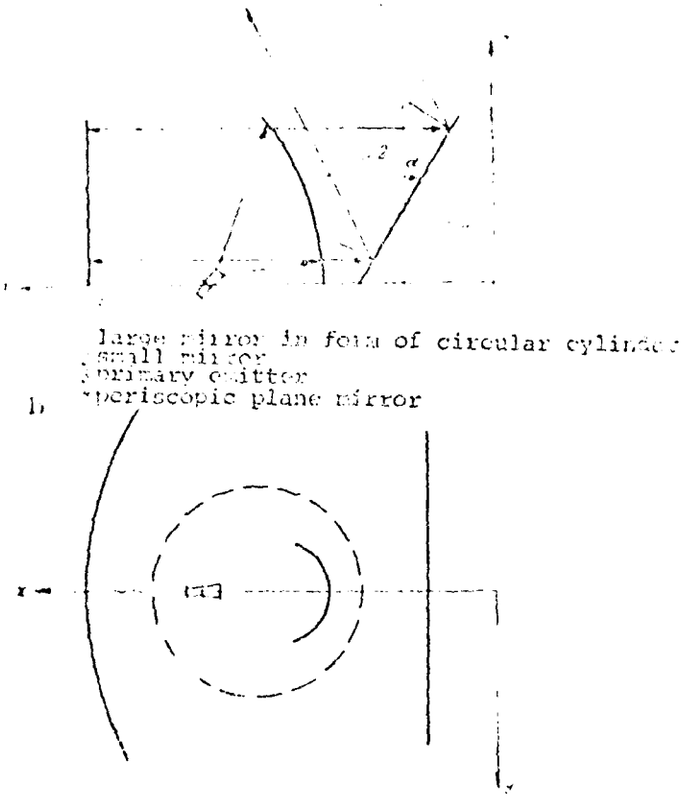
large mirror in form of circular cylinder
small mirror
primary emitter
periscopic plane mirror

Figure 2.

functions given in the paper are limited by the case when the aperture of the small mirror comprises 0.05 of the diameter of the large mirror. The possibilities of further reducing the dimensions of the small mirror will be considered in this paper, which may be necessary when developing very large instruments of both the spherical and cylindrical type. Moreover, a method of calculating the small mirror for a cylindrical two-mirror system is presented in this paper and a number of practical instructions is given on selecting the mutual position of its components.

Dependence of the Geometric Utilization Factor on the Position and Value of the Aperture of the Small Mirror

Let us recall that the ratio of the existing aperture of the large mirror D_p to its total diameter D_0 is called the geometric utilization factor:

$$K_r = \frac{D_p}{D_0} = \frac{R_{y\,p.c.}}{R_0}.$$

Further, for generality, let us assume that $R_0 = 1$ and let us find the results expressed in fractions of a radius. The function of interest can easily be found by making use of parametric equations of the focal curve at $R_0 = 1$:

$$Y = \sin^3\varphi, \quad X = \cos\varphi\left(1 - \frac{\cos 2\varphi}{2}\right). \tag{1}$$

Actually, let us consider Figure 3 where the horizontal cross-section of the large mirror and its focal curve are shown. Let us initially consider the case when the small mirror is located in the prefocal zone. The position of its aperture is denoted by 1 and the path of the beams in the antenna is shown by the dashed line. It is easy to see that coordinates Y and X of the focal curve are coordinates of the extreme points of the aperture of the small mirror and correspondingly angle φ corresponding to them immediately determines the value of the effective aperture of the large mirror:

$$K_r = \sin\varphi = K_{y\,p.c.}$$

at $R_0 = 1$;

$$Y = F_{p.s.} \sin^2\varphi_1,$$
$$X = F_{p.s.} \cos\varphi_1 \left(1 - \frac{\cos 2\varphi_1}{2}\right).$$

When the small mirror is located in the transfocal zone (the position of its aperture is denoted by 2), the path of the beams in the antenna is shown by the solid line. The extreme point of the aperture of the small mirror coincides with the point of intersection of the reflected beam with its opposite branch rather than with the point of contact of the reflected beam with the focal curve.

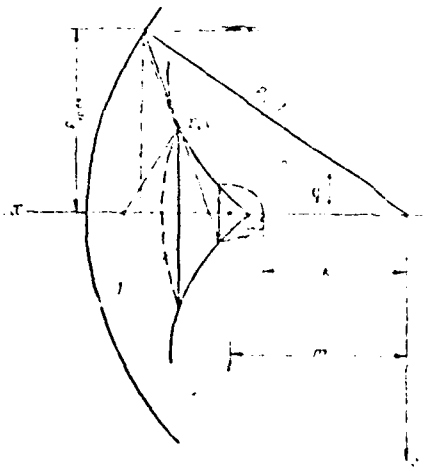

Figure 3

The following transcendental equation must be solved to establish the function of interest:

$$\frac{\cos\varphi - \cos\varphi_1\left(1 - \frac{\cos 2\varphi_1}{2}\right)}{\sin\varphi - \sin^2\varphi_1} = \frac{\cos\varphi - \cos\varphi_2\left(1 - \frac{\cos 2\varphi_2}{2}\right)}{\sin\varphi - \sin^2\varphi_2}, \tag{2}$$

where

$$\cos\varphi_1\left(1 - \frac{\cos 2\varphi_1}{2}\right) = \frac{R_{sp.s.}}{\sin^2\varphi_1} = R_{s.p.m.}$$

This is easy to do by resorting us, for example, of the graphical method of solution. The function $k = f(D_{sp}/R_0)$ is presented in figure 4 for the prefocal and transfocal zones (curves 1 and 2). Curve 3 [illegible] which determines the position of the aperture of the small mirror, is presented here also.

It is obvious from the curves (1 and 2) that transfocal mirrors have undoubted advantages over prefocal mirrors since they provide a considerably greater value of k with identical apertures of the small mirrors.

Let us consider the possibility of realizing small mirrors with dimensions $D_{sp} < 0.05\ D_0$ in the transfocal zone.

It is first required that the small mirror not intersect the focal curve. To do this, its vertex should be located behind the paraxial focus, i.e., $k < 0.5$.

Since c is the common path of the central beam from the emitter to the reflected wave front:

$$c = 1 + m - 2k, \tag{3}$$

where m is the distance from the center of the mirror to the emitter, then the inequality $c > m$ should be fulfilled in this case.

Let us investigate its fulfillability. For us write an expression that permits one to determine the path c for a beam passing through the extreme point of the aperture of the small mirror:

$$c = \sqrt{(m - R_{sp}\cos\varphi)^2 + R_{sp}^2\sin^2\varphi} + \sqrt{(R_{sp}\cos\varphi - R_{sp}\cos\varphi)^2 + (R_{sp}\sin\varphi - R_{sp}\sin\varphi)^2} + \\ + (1 - R_{sp}\cos\varphi). \tag{4}$$

The values of $R_{sp}\cos\varphi$, $R_{sp}\sin\varphi$, $R_{sp}\cos\varphi$, and $R_{sp}\sin\varphi$ contained in the expression for c are determined by means of curves 1 and 3 in Figure 4.

The value of m is determined at which the condition $c > m$ is fulfilled.

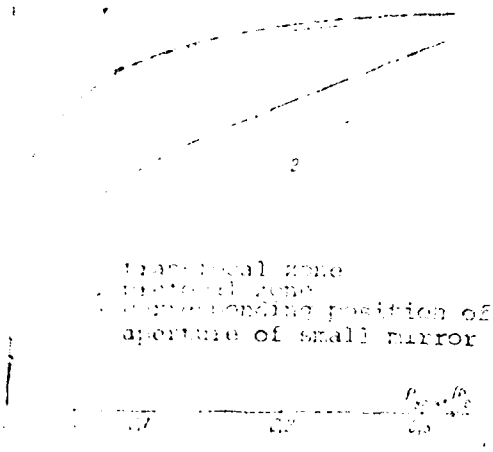

Figure 4.

that the maximum values of the geometric utilization factors cannot be realized for apertures of $D_{p\ min} < 0.05\ D_0$ since the emitter is then submerged inside the mirror and the required angle of small mirror rotation on the order of 300°, which is difficult to realize. If radiation is limited to 160-200°, i.e., if the emitter leaves the aperture of the small mirror, the latter must be moved and the geometric utilization factor K_f decreases.

The behavior of the geometric utilization factor K_f^* is presented in Fig. 5 which corresponds to this circumstance (curve 1). The dependence of the geometric utilization factor K_f (curve 3), previously represented by curve 3 in Fig. 4, is presented here for comparison. Curves 2 and 4 in this figure show the corresponding position of the aperture of the small mirror.

Calculation of the Small Mirror for a Cylindrical Two-Mirror Antenna

The initial position of the generatrix of a cylindrical two-mirror antenna of the parabolic type is selected according to the given conditions of the problem, i.e.,

---

1/ Impossible to intersect the focal curve.

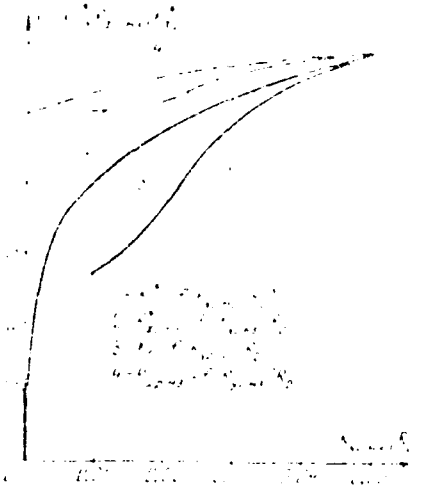

Figure 5.

with respect to the following additional circumstance. Since the small mirror has a profile in the form of an asymmetrical parabola in the vertical cross-section, one must ensure that its upper edge also not intersect the focal curve.

To do this, the condition which is explained by Figure 6 should be fulfilled:

$$m \geq \frac{x^2}{4(0{,}5 - z)} + k, \tag{5}$$

where x is the height of the small mirror.

Let us now turn to finding the surface of the small mirror. It is known that the small mirror in spherical two-mirror antennas is a surface of rotation and the problem reduces to the plane problem, i.e., to finding the profile of the [illegible] ation. In the considered case the small mirror is a surface of double curvature and the problem must be solved in a three-coordinate system (Figure 6).

Let us make use of the wave fronts and let us solve the problem of finding the surface of the small mirror in two steps:

1. By considering the operation of the antenna for reception by the given plane wave front $\bar{x}_1$ impinging on the large mirror $L_{(y)}$, let us determine the reflected wave front $\bar{y}$.

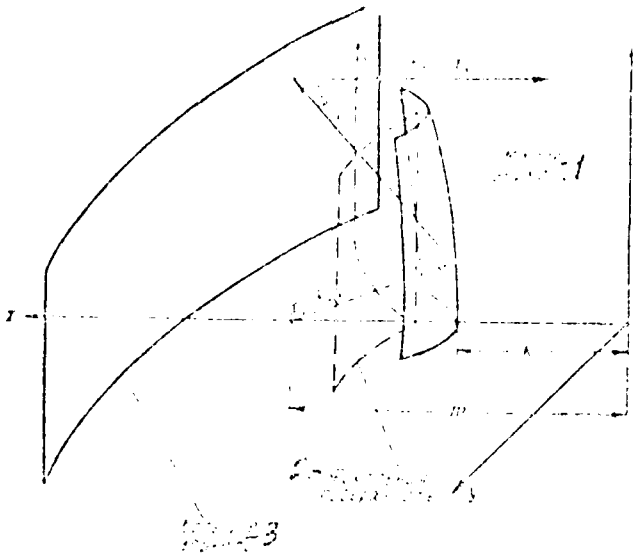

Figure 6.

1—Small mirror. 2—Focal surface. 3—Large mirror

2. By considering the operation of the antenna to transmit by the given wave front $\bar{X}_2$ impinging on the small mirror from the emitter and by the reflected front $\bar{Y}$ determined from the first step, the surface of the small mirror $\bar{R}_{e_2}$ is found.

The equation of the reflected wave front has the following vector form:

$$\bar{Y} = \bar{X}_1 + \bar{\rho}_1 [\bar{n}_1 (\bar{R}_{e_1} - \bar{X}_1)] \tag{6}$$

where

$$\left.\begin{aligned} \bar{X}_1 &= i + yj + zk && \text{equation of incident plane front} \\ \bar{R}_{e_1} &= \bar{l}(\bar{l}\cdot\bar{p}\bar{l}) + \bar{m}(\bar{m}\cdot\bar{p}\bar{l}) + \bar{n}(\bar{n}\cdot\bar{p}\bar{l}) && \text{equation of surface of large mirror} \\ \bar{n}_1 &= \bar{l}(\bar{l}\cdot\bar{p}\bar{l}) + \bar{m}(\bar{m}\cdot\bar{p}\bar{l}) + \bar{n}(\bar{n}\cdot\bar{p}\bar{l}) && \text{equation of normal to surface of large mirror} \end{aligned}\right\} \tag{7}$$

Having substituted (7) into (6), we find the following formulas to determine the coordinates of the reflected wave front:

$$\left.\begin{aligned} Y_x &= [illegible] \\ Y_y &= [illegible] \\ Y_z &= z \end{aligned}\right\} . \qquad (8)$$

The equation of the surface of the small mirror in vector form is

$$\bar{R}_M = \bar{Y} + \bar{r}\,\frac{[c^2 - (\bar{Y} - \bar{X}_2)^2]}{2[c - (\bar{Y} - \bar{X}_2)\bar{r}]}, \qquad (9)$$

where c = 1 + m - 2k is a constant;

$\bar{r} = [1 - 2(1 - \mu^2)]\bar{i} + [-2\mu\sqrt{1 - \mu^2}]\bar{j}$	equation of normal to reflected front	
$\bar{X}_2 = m\bar{i}$	equation of spherical front from emitter subtended to point	(10)

Having substituted (8) and (10) into (9), we find the following expressions to determine the surface coordinates of the small mirror:

$$\left.\begin{aligned} R_{Mx} &= Y_x + [1 - 2(1 - \mu^2)]P \\ R_{My} &= Y_y + [-2\mu\sqrt{1 - \mu^2}]P \\ R_{Mz} &= Y_z \end{aligned}\right\} \qquad (11)$$

where

$$P = \frac{c^2 - [(Y_x - m)^2 + Y_y^2 + Y_z^2]}{2\{c - (Y_x - m)[1 - 2(1 - \mu^2)] - Y_y[2\mu\sqrt{1 - \mu^2}]\}} .$$

Using the given method, a small mirror having an aperture in the horizontal plane equal to 0.02 of the diameter of the large mirror was calculated. The angle of radiation of the mirror in the horizontal plane is approximately 140° and that in the vertical plane is approximately 45°. The calculated amplitude distribution

in the aperture of the large mirror in the horizontal and vertical planes, respectively, are shown in Figure 7a and b. The amplitude distribution in the E-plane has the form of a two-hump curve. It was assumed in calculating this distribution that a waveguide horn antenna that ensures a level of radiation of the side lobes of 0.05 E$_{max}$ was used as the primary emitter. The aperture distribution shown in Figure 7a and b yields an aperture utilization factor equal to 0.85.

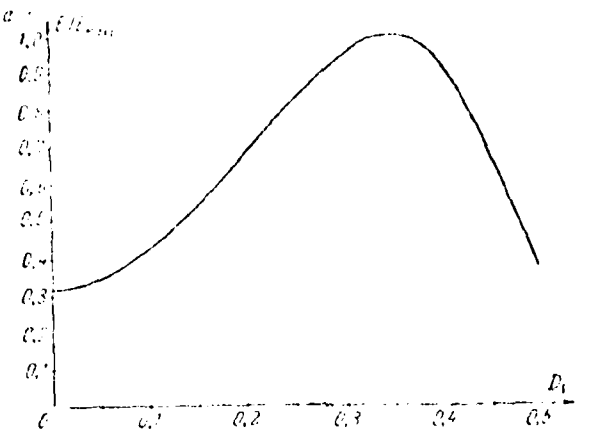

Figure 7a.

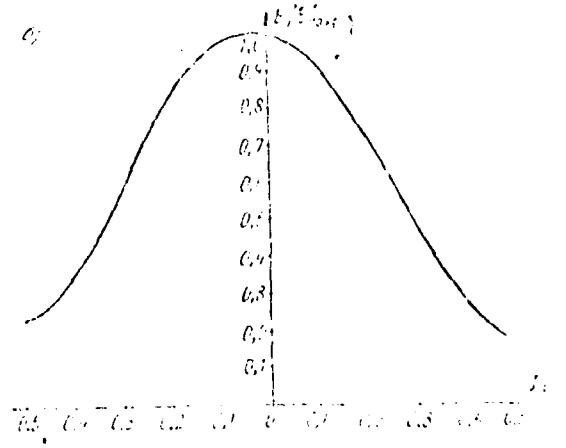

Figure 7b.

Thus, the aperture utilization factor in two-mirror antennas of circular symmetry is rather high even at very low relative dimensions of the small mirror.

Reference

1. [illegible]
2. [illegible]
3. [illegible]

SHAPING THE RADIATION PATTERN OF ARC ANTENNAS 82

V. M. Colovachev and A. A. Kuz'min

A formula was derived to calculate the radiation pattern of arc antennas in the plane of the orthogonal plane of the arc. It is shown that the shape of the radiation pattern is considerably dependent on the radius of the arc and the amplitude distribution in the orthogonal plane. The characteristics of shaping the radiation pattern of an arc antenna in the plane normal to the plane of the arc are considered.

Introduction

A vast number of papers [1, 2, 3, 4] and so on was devoted during the past decade to investigating the characteristics of circular antenna arrays. This interest is explained by the specific advantages of circular antennas over plane antennas, the main one of which includes the capability of wideangle movement of the radiation pattern without changing its characteristics. However, the characteristics of circular (arc) antenna arrays are considered only in the plane of the arc (the azimuth plane) in the majority of published papers, although the interdependence of the radiation patterns in the plane of the arc and the orthogonal plane to it is also known. This interdependence is manifested in that the arc (circular) antenna array has directional properties in the vertical plane even when nondirectional individual emitters are used in this plane. The indicated directional properties are determined by the vertical radiation pattern corresponding to the

... of an arc (circular) antenna. Therefore one must deal with a radia... ...corresponding to the arc coefficient when shaping the special radia... ... (of type cosec^2, sector, $\cos^2$ and so on) in the vertical plane. ..., the radiation pattern corresponding to the arc coefficient [2] is do... ... the geometric dimensions of the arc (with radius R and aperture of 2β), ... pattern of emitters and the amplitude distribution in the azimuth ..., the formula found in [2] to calculate the vertical radiation pat... ...tically valid only for calculating continuous arc antennas. Problems ... the radiation pattern in the vertical plane of arc antennas with dis... ...tions of emitters are considered below.

... Pattern Corresponding to the Arc Coefficient

8)

...diation pattern through the field of an arc symmetrical with respect to ... an antenna consisting of N emitters having directionality in the ... are $F_0(\cdot)$ and amplitude distribution $\{I_j\}$, is determined by the

$$F(\varphi, \theta) = \sum_{j=-n}^{n} I_j F_0(\varphi - \varphi_j) e^{-i[\psi_j(\varphi,\theta)-\psi_j(\varphi_0,\theta_0)]}, \qquad (1)$$

... the angular distance between emitters and $\psi_j(\varphi, \theta)$ is the phase multi... ... arc antenna.

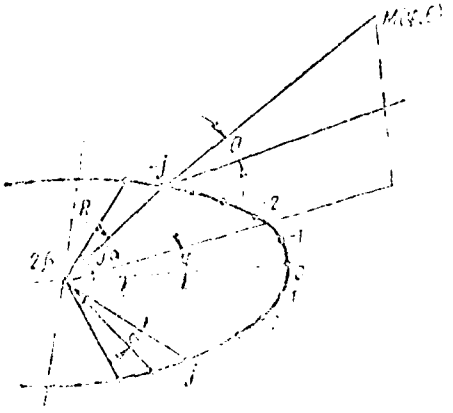

Figure 1.

The expression for phase multiplier $f_j(\varphi, \vartheta)$ of an arc antenna, which can easily be found from figure 1, has the form

$$\xi(\varphi, \vartheta) = kR\cos\vartheta[1 - \cos\alpha_j\cos\varphi + \sin\alpha_j\sin\varphi]. \tag{2a}$$

To ensure cophasal addition of the fields of all emitters in a given direction φ_0, ϑ_0, the electric phase compensation for the j-th emitter should be equal to

$$\xi(\varphi_0, \vartheta_0) = kR\cos\vartheta_0[1 - \cos\alpha_j\cos\varphi_0 + \sin\alpha_j\sin\varphi_0]. \tag{2b}$$

where φ_0, ϑ_0 are angles that determine the direction of the maximum radiation pattern of an arc antenna and R is the radius of the arc.

Consequently,

$$\xi_j(\varphi, \vartheta) - \xi_j(\varphi_0\vartheta_0) = kR[1 - \cos\alpha_j](\cos\varphi\cos\vartheta - \cos\varphi_0\cos\vartheta_0) + \\ + \sin\alpha_j(\sin\varphi\cos\vartheta - \sin\varphi_0\cos\vartheta_0)]. \tag{3}$$

However, the main beam must be moved only in the azimuth plane (plane of the arc) for most practically realizable cases; therefore, one can assume that $\vartheta_0 = 0$. 8-1

To simplify analysis of the radiation pattern in the plane of the normal plane of the arc (in the vertical plane), which is of interest at a given moment, let us assume that the maximum main beam in the orthogonal plane has direction $\varphi_0 = 0$. The radiation pattern in the vertical plane corresponding to the arc coefficient is then written as

$$F(\vartheta) = \sum_{j=-n}^{n} I F_u(\alpha_j)\exp\{ikR(1 - \cos\alpha_j)(1 - \cos\vartheta)\}. \tag{4}$$

Multiplier $I_u(\alpha_j)$ in expression (4) determines the contribution of the arc to the radiation field due to the directional properties of the emitters in the azimuth plane in direction $\varphi = 0$. It is obvious that this multiplier will be determined by a function which characterizes the radiation pattern of an emitter in the azimuth plane and that it will fulfill the role of weight to the amplitude distribution. Let us rewrite formula (4) in the form

$$F(u) = e^{-iu} \sum_{j=-n}^{n} I_j \exp[iu\cos \alpha_j], \tag{5}$$

[illegible] is a generalized coordinate and $\{I_j\} = \{I\} I_n(\alpha)$ is [illegible] amplitude distribution in the plane of the arc. Then, using the equality

$$[illegible] = \sum_{-\infty}^{\infty} i^l J_l(u) \exp(i l \alpha_j),$$ we find

$$F(u) = \sum_{j=-n}^{n} I_j \sum_{l=-\infty}^{\infty} i^l J_l(u) \exp(i l \alpha_j). \tag{6}$$

[illegible] expression (6) that the vertical radiation pattern of an arc an[illegible] as the horizontal pattern, is complex in nature and has no zeros [illegible] case.

[illegible] of an arc antenna are isotropic and uniformly excited, i.e., [illegible], the expression for the vertical radiation pattern then assumes [illegible]

$$F(u) = \sum_{l=-\infty}^{\infty} i^l J_l(u) \sum_{j=-n}^{n} \exp(i l \alpha_j). \tag{7}$$

[illegible] that [illegible] $\frac{\beta}{\lambda}$ and $\sum_{j=-n}^{n} \exp(i l \alpha_j) = \frac{\sin l\beta}{\sin l \frac{\beta}{\lambda}}$,

[illegible] finally find

$$F(u) = J_0(u) + \sum_{l=-\infty}^{\infty}{}' i^l J_l(u) \frac{\sin l\beta}{\lambda \sin l \frac{\beta}{\lambda}}. \tag{8}$$

[illegible] in summation index l denotes the absence of the value with l = 0 [illegible] summation sign.

It is easy to find the expression from (7) for a complete ring of [illegible] a vertical radiation pattern of form

$$F(u) = J_0(u) + \sum_{n=1}^{\infty} i^n J_n(u) \tag{9}$$

In the case when a circular array with sufficiently large number of emitters N is used such that $N \to \infty$, the vertical radiation pattern of this array is written as

$$F(u) = J_0(u) + 2\sum_{n=1}^{\infty} J_n(kR) \cos n\theta \tag{10}$$

Expression (10) fully coincides with the expression found in [3] for a continuous circular aperture. Moreover, it is easy to show from (9) that the radiation pattern in the vertical plane possesses symmetry at $\theta = 0$, which corresponds to the case of a linear antenna. Let us write down formula (9) for circular antennas with radiating sector $2\theta < \pi$, for which expression (10) is invalid. With a sufficiently large number of emitters N ($N \to \infty$), expression (9) is simplified even more and assumes the form

$$F(u) = J_0(u) + \sum_{n=1}^{\infty} i^n J_n(u) \frac{\sin n\theta}{n\theta} . \tag{11}$$

If one limits oneself to the first few terms of expression (11), then to calculate the width of the radiation pattern of arc antennas in the vertical plane one can make use of the relation

$$2\Delta\theta_{0,5} = \frac{173}{\sin\frac{\theta}{2}\, kR} . \tag{12}$$

The accuracy of calculation by formula (12) is no worse than $\pm$ 5 percent. It is obvious from expression (12) that the width of the radiation pattern is determined by radius R and the value of the radiating sector 2θ of an arc antenna. The calculated dependence of the width of the radiation pattern of arc antennas on the angular aperture 2θ is presented in Figure 2 for different values of kR. It is obvious from the given curves that the width of the radiation pattern increases significantly when the values of kR are reduced, especially for small values of aperture 2θ of arc antennas. From the physical viewpoint, this is explained by a decrease of the value of phase θ as determined by the configuration of arc antennas.

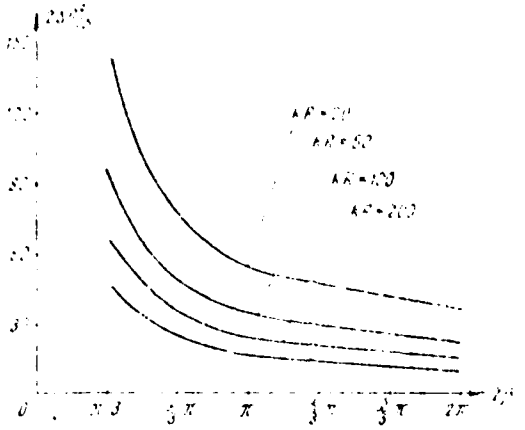

Figure 2.

Results of Calculation

A number of numerical calculations was made to investigate the variation of [illegible] of the vertical radiation pattern of arc antennas at different amplitude distributions in the plane of the arc by formulas (1) and (6). Calculations by formula (1) were also made on a Ural-2 computer and those by formula (6) were made manually. Good agreement of the points calculated on a digital computer and manually is obvious from the patterns given below (see Figure 3) (the calculated points by formula (6) are noted on the diagrams by the points).

The calculated radiation patterns [illegible] illustrate the effect of different amplitude distribution for arc antennas with curvature determined by the values kR = 10 and kR = 150 and with angular extensions of 2Φ = 90, 135 and 180° are presented in Figures 3-8.

It is obvious from consideration of the figures that the shape of the vertical radiation pattern corresponding to the [illegible] of the antenna is close to cosecant. This is explained by the fact that [illegible] by virtue of the difference of the beam path from different segments of the arc with respect to plane Φ = 0 is insignificant at small angles of [illegible] and the radiation field is almost equal to the maximum value. [illegible] with

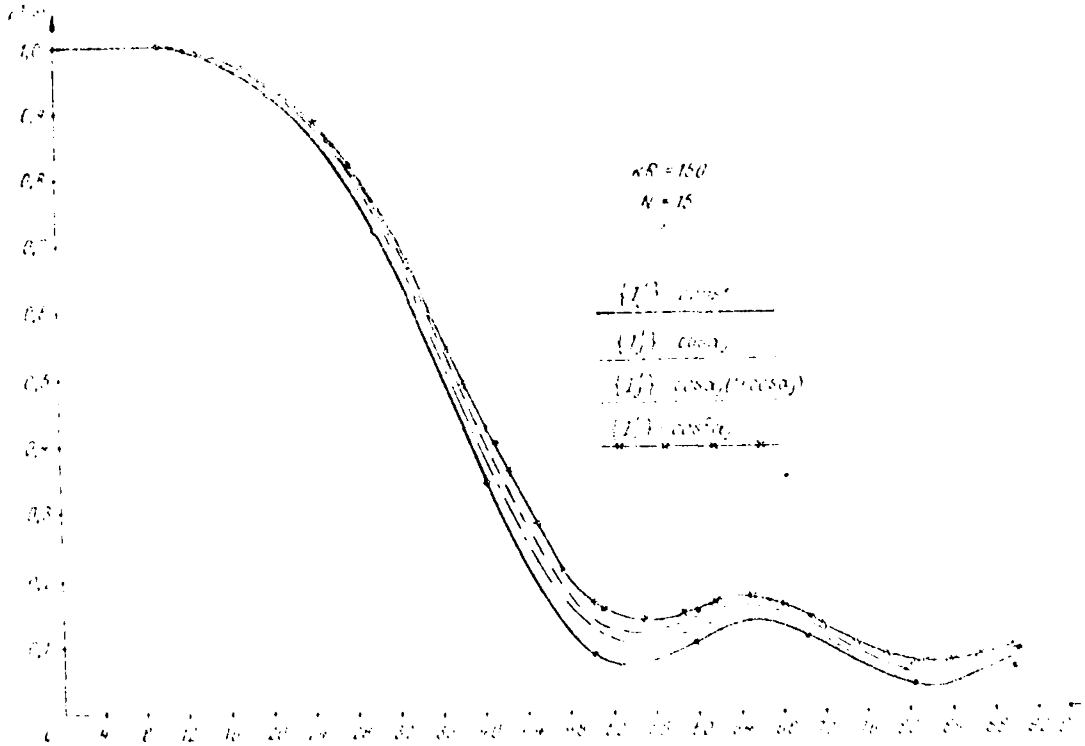

Fig. 3.

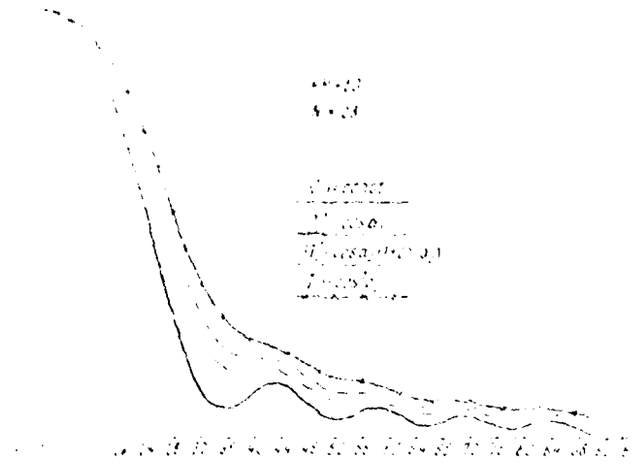

Figure 4.

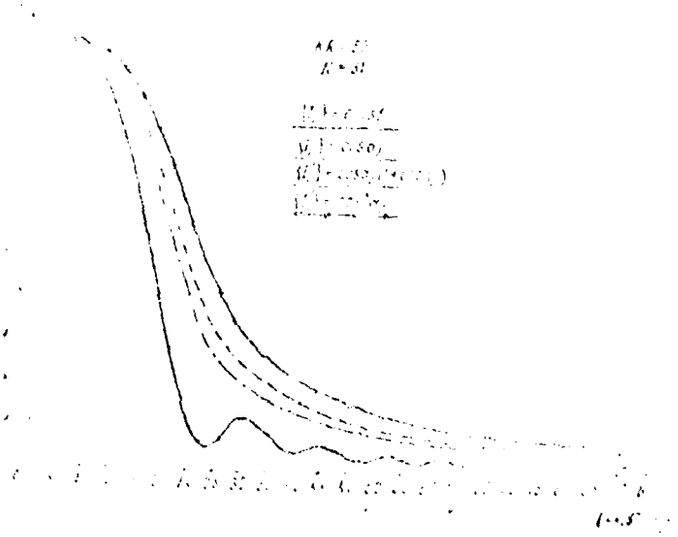

Figure 5.

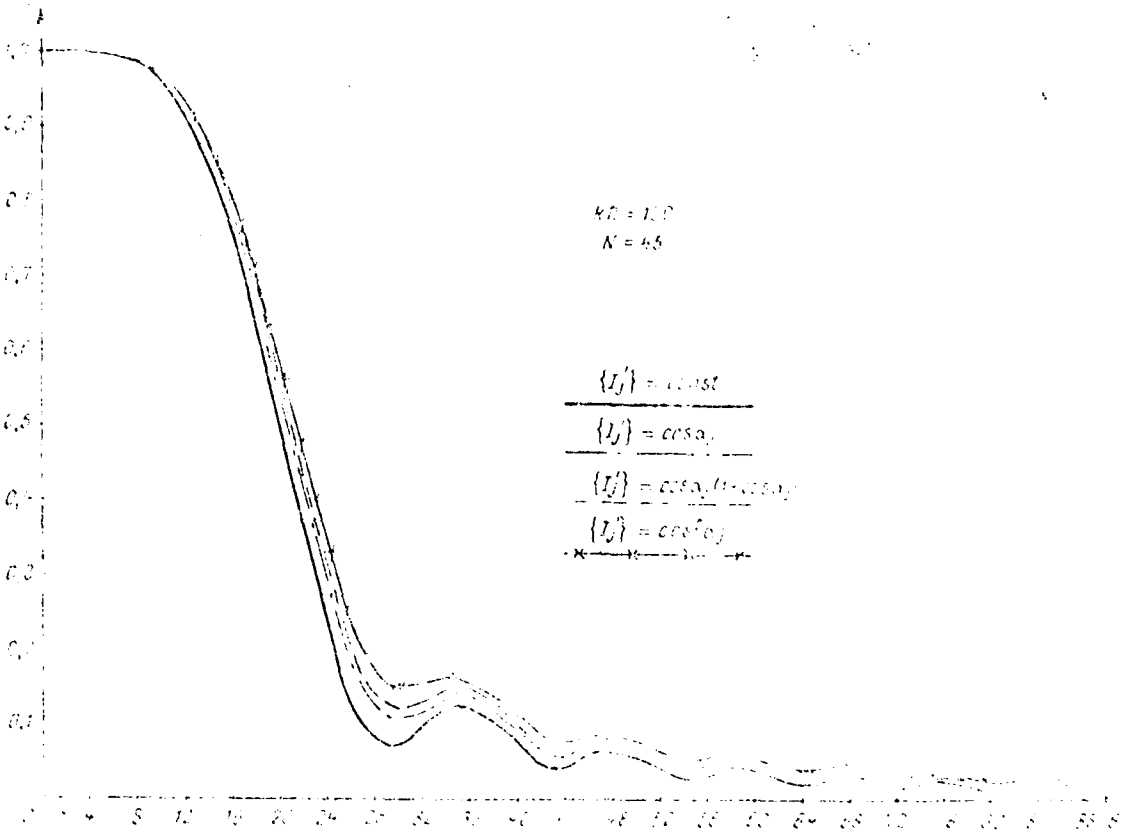
$\{I_j\} = const$
$\{I_j\} = \cos\alpha_j$
$\{I_j\} = \cos\alpha_j(1+\cos\alpha_j)$
$\{I_j\} = \cos^2\alpha_j$

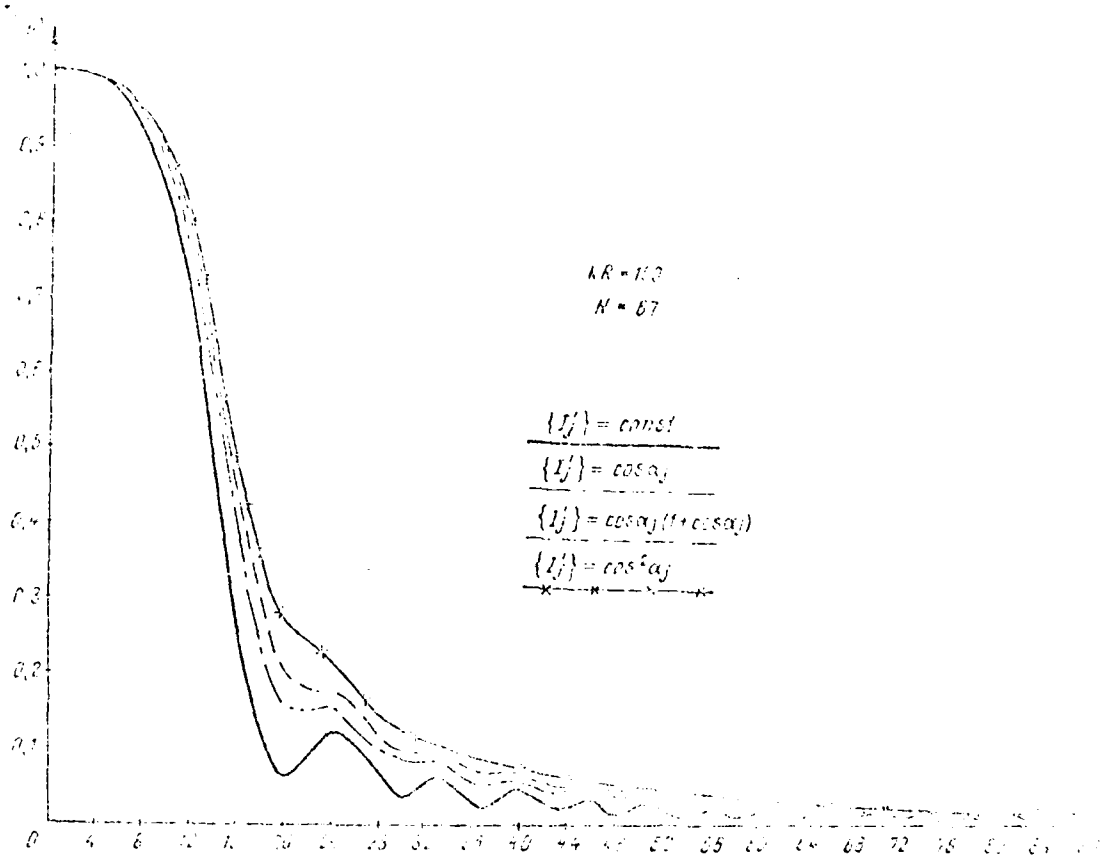

Fig. 7.

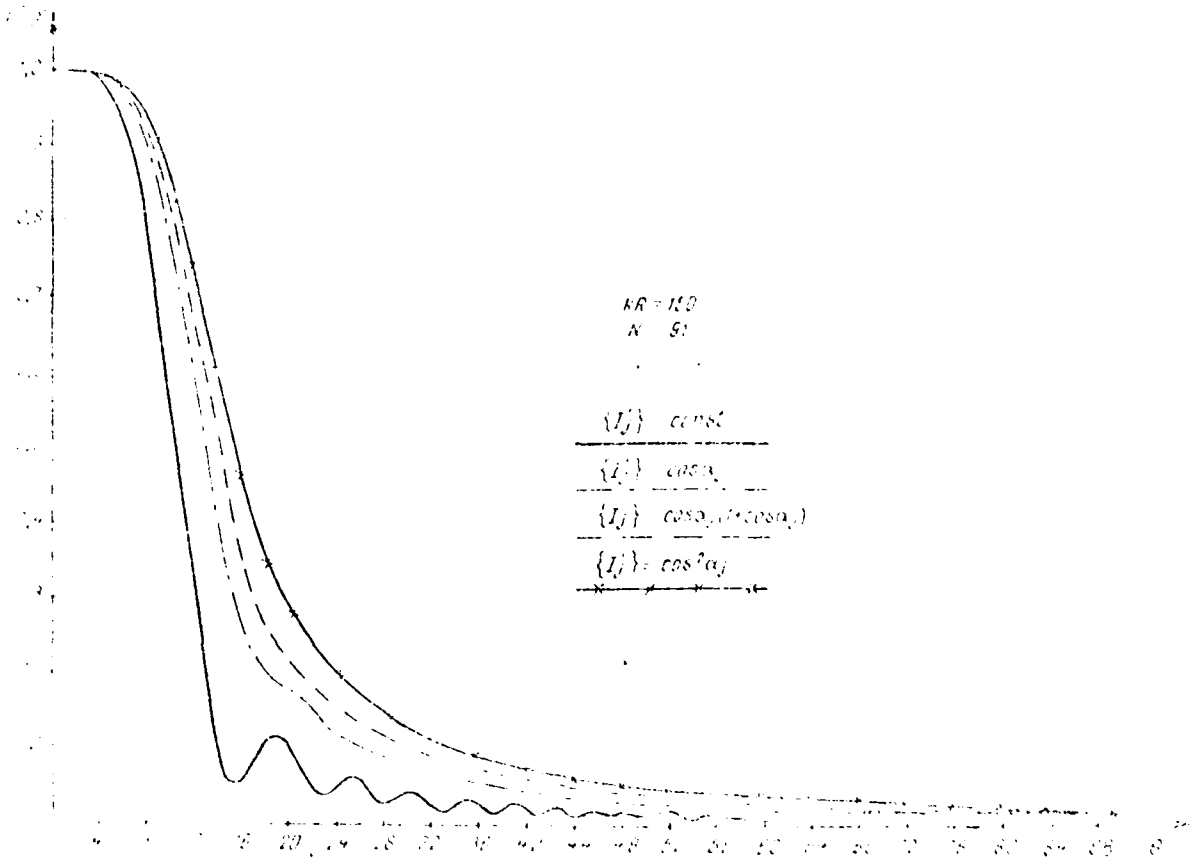

Fig. 8.

further increase of angles θ and the field drops sharply in the far zone. The presence of nonuniform amplitude distribution in the plane of the arc leads to expansion of the radiation pattern in the orthogonal plane due to a decrease of the contribution of radiation to the total field from components located on the edges of the aperture. Moreover, as indicated above, the radiation patterns have no zeros and a gradual transition from the vibrational process of signal variation beyond the main lobe to smooth "pulling" of its slope is observed with an increase of nonuniformity of amplitude distribution. Some steadiness of the shape of the radiation pattern with respect to the type of amplitude distribution is observed at relatively small angular apertures ($2\theta_0 \leq 90°$) of an arc antenna. This occurs due to a reduction of the nonuniformity of amplitude distribution within small aperture angles $2\theta_0$ of an arc antenna and its approach to a linear antenna in which the radiation pattern in the vertical plane is generally independent of the amplitude distribution in the azimuth plane.

Thus, it follows from the previous section and analysis of the calculated radiation patterns corresponding to the arc coefficient that an arc array consisting of emitters nondirectional in the vertical plane has directional properties. The latter circumstances places specific requirements on the shaping of the radiation patterns of arc arrays required in the vertical plane, especially in shaping wide-directional patterns or patterns of special shape (cosec$^2\theta$, sector and so on).

Characteristics of Shaping a Given Radiation Pattern in the Vertical Plane in Arc Antennas

The radiation patterns in both the plane of the arc and in the orthogonal to it are usually given when designing arc antenna arrays. The geometric dimensions of the arc (radius R and aperture $2\theta_0$) and also the required total amplitude distribution $\{I_j\}$ are determined by the given characteristics of the radiation pattern in the plane of the arc--width, level of side lobes, scanning sector and so on.

The procedures are usually used to calculate the vertical radiation pattern corresponding to the coefficient of an arc antenna array. Refs. [3, 7] can be used for this. Let us gain an insight into the vertical radiation patterns

... to the coefficient of an arc antenna array consisting of nondirec-
... in the vertical plane were considered in previous sections. The
... directional in antennas have specific directionality in both planes
..., ... with a sufficient degree of accuracy for most practical
... equation of an emitter is represented in the form:

$$I_{...}(\varphi, \theta) \quad f(\varphi) F_1(\theta, \quad (13)$$

... radiation pattern of an emitter in the plane of the arc, $F_1(\theta)$ ...
... pattern of an emitter in the plane of the normal plane of the arc
... determined by direction cosines.

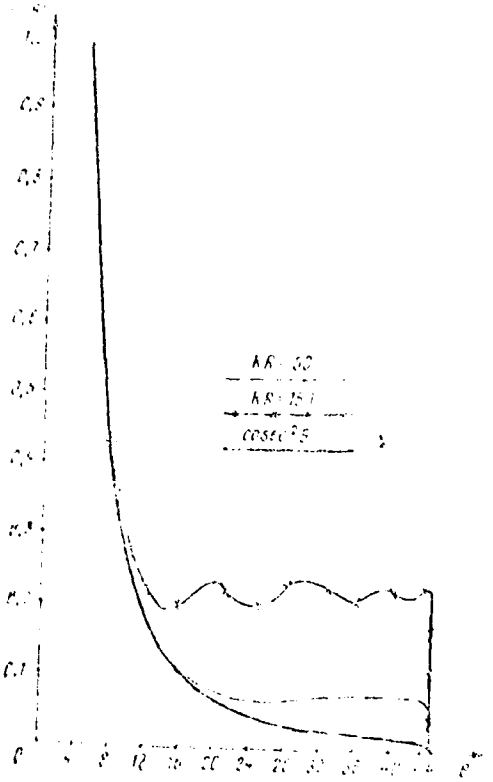

Figure 9.

... (13) ... we see that the ... emitters are ... in different cross-sections ..., i.e.,

$$I_1(\theta) \quad I_2(\theta) \quad \ldots \quad I_n(\theta,$$

and the total (required) radiation pattern in the plane under consideration is written in the form

$$G(\varphi) \quad F(\varphi) F_1(\varphi), \tag{13a}$$

where $G(\varphi)$ is the required radiation pattern in the vertical plane, $F_1(\varphi)$ is the radiation pattern in the vertical plane of an individual emitter and $F(\varphi)$ is the vertical radiation pattern corresponding to the coefficient of an are array, calculated by formula (6). It follows from expression (13a) that to obtain the required vertical radiation pattern in an arc antenna one must see that the radiation pattern of the individual emitter satisfies the condition

$$F_1(\varphi) \quad \frac{G(\varphi)}{F(\varphi)}. \tag{14}$$

It is obvious that the form of the radiation pattern $F_1(\varphi)$ of an individual emitter will be determined both by the geometric dimensions of the arc and by the shape of the required radiation pattern.

Variation of the shape of the vertical radiation pattern in power $F_1(\varphi)$ of an individual emitter installed in an arc antenna with geometric dimensions of 2Φ = = 135°, kR = 50 and 150 and $\{I_j'\} = \cos^2\varphi_j$ for shaping a radiation pattern variable in sector $5° \leq \theta \leq 45°$ by the law $\cos^2\theta$ is presented for illustration in Figure 8. An ideal radiation pattern (solid curve) of type $\cos^2\theta$, which should be formed by an emitter located in a linear antenna array, is presented for comparison in the same Figure 9. The results given in Figure 9 confirm the foregoing, namely that the shape of the corresponding radiation pattern of an individual emitter can vary significantly when shaping wide-directional radiation patterns in arc antennas. The problem further reduces to synthesis of an individual emitter by the given radiation pattern determined by formula (14).

Conclusions

1. In arc antennas consisting of isotropic emitters the directional properties both in the plane of the arc and in the plane orthogonal to it. The derived relations for calculating the radiation patterns of arc

antenna in the plane no[illegible] to the plane of the arc is considerably dependent on [illegible] [illegible]tric dimensions of the arc.

[illegible]. The effect of different amplitude distributions on the radiation pattern [illegible] arc antenna array in the plane of the normal plane of the arc, as indicated [illegible] calculations, becomes appreciable with angular antenna aperture of [illegible].

[illegible]. The radiation patterns of the entire antenna and of the individual emitter [illegible] plane of the normal plane of the arc differ considerably, which should be taken [illegible] when designing arc antennas with radiation patterns of special sha[illegible] [illegible] indicated above.

References

1. [illegible] Л. Н. Коммутационные антенны с [illegible]. Известия вузов СССР. Радиотехника, [illegible]
2. [illegible] Л. Н., [illegible]енко А. Н. Диаграммы [illegible] антенных решеток. Известия вузов СССР. Радиотехника, [illegible] т. VIII, № [illegible], стр. 574–580.
3. [illegible] F. G. Limitations on Directional Patterns of Phase-compensated Cir[illegible] Arrays. The Radio and Electronic Engineers, Oct. 1965, vol. 30, № [illegible] [illegible] 22.
4. [illegible] P. W. Polar patterns of phasecorrected circular arrays. Electr[illegible] [illegible], Oct. 1965, № 1[illegible]

ENERGY CHARACTERISTICS OF PERIODIC SYSTEMS OF EMITTERS

I. V. Guseyev and A. V. Kolot

Expressions are derived in this paper, which is a continuation of [1], for the efficiency and efficiency factor. The relationship between the scattering matrix and the partial amplification of the array component was established.

The Efficiency and Power Efficiency Factor, the Front-to-Rear Factor and the Amplification Factor

The efficiency for a linear periodic array with several active emitters whose feeders are excited by outside incident waves is equal to

$$\eta = \frac{W_{rad}}{W_{in.p}} = \frac{\sum_{n=-\infty}^{\infty} (|a_n|^2 - |b_n|^2)}{\sum_{p=p_1, p_2, \ldots, p_\alpha} |a_p|^2}, \qquad (1)$$

where $p_1, p_2, \ldots, p_\alpha$ are the numbers of the active emitters of the array and a_p and b_p are the complex amplitudes of direct and reverse waves in the p-th feeder line of the emitters.

Based on [2] and using Parseval's theorem, one can give relation (1) in the form

$$\eta = \frac{1}{g_1} \frac{\int_{-\pi}^{\pi} |\tilde{a}(u)|^2 (1 - |\Gamma(u)|^2) du}{\sum_{p=p_1, p_2, \ldots, p_\alpha} |a_p|^2}, \qquad (2)$$

... $\tilde{s}(u)$ and $\tilde{s}(u)$ are complex Fourier series consisting of the amplitudes of ... (s_{ij}) and of components of the central line of the scattering matrix ... , respectively (see [1]).

... the emitter and an identical load of the feeder lines of passive com... characterized by reflection factor Γ are excited, based on [1] and formu...

$$\dots = \dots \frac{2\pi \dfrac{\displaystyle\int_{-\pi}^{\pi} \frac{1 - |\tilde{s}(u)|^2}{|1 - \Gamma\tilde{s}(u)|^2}\, du}{\left|\displaystyle\int_{-\pi}^{\pi} \frac{du}{1 - \Gamma\tilde{s}(u)}\right|^2}}{\dots} \dots \quad (p = 0, \pm 1, \dots). \tag{3}$$

... load of the feeder lines of passive components ($\Gamma = 0$), from (3) 97 ... relation

$$\dots = 1 - \frac{1}{2\pi}\int_{-\pi}^{\pi} |\tilde{s}(u)|^2\, du = 1 - \sum_{n=-\infty}^{\infty} |s_n|^2 \quad (p = 0, \pm 1, \dots). \tag{4}$$

... to that found in [2] for two-dimensional periodic arrays.

... consider the case when emitters with numbers in the range of $-N \le n \le N$ ... linear phase distribution while the feeder lines of the remaining ... loaded by their wave impedance, i.e.,

$$a_n = \begin{cases} |a_n| e^{-jn\beta}, & n = 0, \pm 1, \pm 2, \dots \pm N; \\ 0, & n = \pm(N+1), \pm(N+2), \dots \end{cases} \tag{5}$$

... the phase difference between ... differs.

... periodic function $|\tilde{s}(u)|^2$ ... $|s_n|$ ($n = \dots$) ... sufficiently ... $|s_n|$ ... and has a single ... in the ... ($u = \dots$) in $(0, \pi)$ ... $(-\pi, 0)$. ... this fact alone and ... , based on (3) ...

... relation (6) becomes precise in the range of $N \to \infty$.

$$\eta(\Phi) \sim 1 - |\tilde{s}(\Phi)|^2 \qquad (6)$$

The [illegible] power (W_{rad}) is a function of characteristics [illegible] the antenna and sources that are a [illegible] system; therefore, variation of $W_{r.a}$ can [illegible] characterized by the so-called power efficiency factor rather than the efficiency, which is a characteristic of the antenna only,

$$\xi = \frac{W_{r.a}}{W_{\text{макс}}}, \qquad (7)$$

where $W_{\text{макс}}$ is the maximum possible total power which can be taken from sources that excite the system.

If the sources are voltage generators with electromotive force $\mathcal{E}_n$ and with identical internal impedance characterized by reflection factor Γ, then on the [illegible] of (7), using the Parseval identity, we find[2/]:

$$\xi = (1 - |\Gamma|^2)\frac{\displaystyle\int_{-\pi}^{\pi} \frac{1 - |\tilde{s}(u)|^2}{|1 - \Gamma\tilde{s}(u)|^2} |\tilde{\mathcal{E}}(u)|^2 du}{\displaystyle\int_{-\pi}^{\pi} |\tilde{\mathcal{E}}(u)|^2 du}, \qquad (8)$$

[illegible] of electromotive force [1].

If the array is excited by $(2N + 1)$ voltage generators with linear phased [illegible] (4)), then with the same assumptions as in derivation of (6), we find

$$\xi(\Phi) \sim (1 - |\Gamma|^2)\frac{1 - |\tilde{s}(\Phi)|^2}{|1 - \Gamma\tilde{s}(\Phi)|^2}. \qquad (9)$$

[2/] [illegible] recall that the voltage source [illegible] maximum possible output on a load [illegible] coupled to the internal impedance of the source.

... factor coincides with efficiency which is natural ... waves are not dependent on losses due to the absorption in the generators.

... linear periodic array using the notations of [1], relations ... are replaced by the following:

$$\sigma_{ij} = \sigma_{ij}^{(1)} = 4\pi^2 \frac{\int_{-\infty}^{\infty}\int_{-\infty}^{\infty} \frac{1-|\tilde{s}(u,v)|^2}{|1-\Gamma\tilde{s}(u,v)|^2} e^{-2\pi i(ui+vj)}\,du\,dv}{\left|\int_{-\infty}^{\infty}\int_{-\infty}^{\infty} \frac{e^{-2\pi i(ui+vj)}\,du\,dv}{1-\Gamma\tilde{s}(u,v)}\right|^2}, \quad (10)$$

$$\sigma_{ij} = 1 - \frac{1}{4\pi^2}\int_{-\infty}^{\infty}\int_{-\infty}^{\infty} |\tilde{s}(u,v)|^2 e^{-2\pi i(ui+vj)}\,du\,dv - 1 - \sum_{n=-\infty}^{\infty}\sum_{m=-\infty}^{\infty} s_{nm} s_{n-i,m-j}^{*} \quad (11)$$

$$\gamma_1(\Phi, \Psi) \simeq 1 - |\tilde{s}(\Phi, \Psi)|^2, \quad (12)$$

$$\xi(\Phi, \Psi) \simeq (1-|\Gamma|^2)\frac{1-|\tilde{s}(\Phi,\Psi)|^2}{|1-\Gamma\tilde{s}(\Phi,\Psi)|^2}. \quad (13)$$

Let us turn to a linear or two-dimensional periodic array with a single active emitter and with wave loads in the feeder lines of the passive components. Setting the expressions for radiative power calculated by the fields in the far zone and in the feeder lines of the system equal and using [1], one can find the equality

$$\eta^{(\omega)} = \int_{\theta=0}^{\pi}\int_{\varphi=0}^{2\pi} |f^{(\omega)}(\theta, \varphi)|^2 \sin\theta\, d\theta\, d\varphi, \quad (14)$$

where $f^{(\omega)}(\theta, \varphi)$ and $\eta^{(\omega)}$ are the partial pattern and efficiency of the component for linear and two-dimensional arrays, respectively.

Denoting the front-to-rear factor of the component of the array by $D^{(\omega)}(\theta, \varphi)$ (with overload of the passive feeder lines) and relying on the determination of front-to-rear factor, we find

$$D^{(\omega)}(\theta, \varphi)\eta^{(\omega)} = 4\pi\left|f^{(\omega)}(\theta, \varphi)\right|^2 = P^{(\omega)}(\theta, \varphi). \quad (15)$$

where $F^{(e)}(\theta, \varphi)$ is the amplification of the component of linear or two-dimensional arrays (with wavelead of feeder lines).

Relations (14) and (15) can be regarded as conditions for normalization of partial patterns.

Let us note in concluding the section that the relationship between efficiency, front-to-rear factor, amplification and the partial pattern of the component in an array with arbitrary, but equal loads in the feeder lines retains the form of equalities (14) and (15) in which it is thus sufficient to replace superscript (e) by (o) [3].

Relationship Between Scattering Functions and Partial Amplification of the Component in a Periodic Array

The power emitted by an antenna system can be calculated doubly: by the wave amplitudes in the feeder lines and by the fields in the far zone.

Since the wave amplitudes are related by the scattering matrix and the radiation fields are expressed by superposition of partial patterns, it becomes possible to establish the relationship between these most important characteristics of the system. Relations were found in [3, 4] between the wave amplitudes in the feeder lines and the emitted power for the final systems of the emitters. Applying these relations to linear periodic systems of emitters and taking their characteristics into account [1]:

$$S_{nm} = s_{|n-m|}, \quad s_l(n, m, p = 0, \pm 1, \pm 2, \ldots),$$
$$\vec{f}_p^{(e)}(\theta, \varphi) = \vec{f}_0^{(e)}(\theta, \varphi) \exp(ip\psi_0 \cos\theta),$$

one can find the equalities

$$Q_q = \sum_{l=-\infty}^{\infty} s_l s_{l+q}^* \quad (q = 0, \pm 1, \pm 2, \ldots); \tag{26}$$

$$\gamma_q = \int_{\varphi_1}^{\varphi_2} \int_0^{\pi} \left| \vec{f}_0^{(e)}(\theta, \varphi) \right|^2 \exp(-iq\psi_0 \cos\theta) \sin\theta \, d\theta \, d\varphi \tag{27}$$

in which $q = m' - m$, $Q_{\ldots} = Q_{\ldots}(\ldots, t, \ldots)$, i.e., the components of infinite matrices [τ] and [s] are actually dependent on the difference of the superscripts for the array under consideration. For two-dimensional periodic arrays, in lieu of (16) and (17), we have

$$Q_{\alpha\beta} = \sum_{l'=-\infty}^{\infty} \sum_{l=-\infty}^{\infty} s_{ll'} s^{*}_{l-\alpha,\, l'-\beta}(\gamma, \delta) \quad (\alpha, \beta = 0, \pm 1, \pm 2, \ldots), \tag{18}$$

$$\tau_{\alpha\beta} = \int_{\theta=0}^{\pi} \int_{\varphi=0}^{\pi} \left| f^{(0)}_{\alpha\beta}(\theta, \varphi) \right|^2 \exp\{-i\gamma k d_1 \sin\theta\cos\varphi - \\ - i\beta k d_2 \sin\theta \sin\varphi\} \sin\theta \, d\theta \, d\varphi \\ (\alpha, \beta = 0, \pm 1, \pm 2, \ldots), \tag{19}$$

where α and β are the differences of the indices for the lines and columns, respectively.[1/]

The values of τ_q for a linear and $\tau_{\alpha\beta}$ for a two-dimensional array are the coefficients of interaction of the partial patterns of specific emitters of the systems being considered; they differ from similar coefficients introduced in [3, 4] only by the multiplier determined by normalization of the patterns. In this case, according to (16), (17) and (19) the values of τ_0 and τ_{00} have physical meaning of the efficiency of emitters of the corresponding arrays (with wave load of the feeder lines of the remaining components); τ_q (at $q \neq 0$) and $\tau_{\alpha\beta}$ (at $\alpha^2 + \beta^2 \neq 0$) are measures of the nonorthogonal nature of partial patterns.

It is simplest to explain the meaning of the components of infinite matrices [9] for the arrays being considered by relying on relations (22) and (27) (see below), from which analytically follow the almost evident equalities [2, 3, 4]:

1/ Note that it was assumed in deriving relations (17) and (19) that there are no non-decaying surface waves in infinite arrays; in the opposite case they would have to be taken into account in the corresponding sums.

$$Q_0 = \sum_{n=-\infty}^{\infty} \ldots \quad (1 - \ldots)$$

$$Q_{0,1} = \sum_{n=-\infty}^{\infty} \sum_{m=-\infty}^{\infty} \ldots \quad (1 - \ldots)$$

First let us go to a linear array, let us introduce the notations:

$$u = kd\cos\varphi, \tag{20a}$$

$$g(u) = \frac{1}{2\pi}\int_0^{2\pi} g_0(\varphi)\left(\arccos\frac{u}{kd}, \varphi\right)d\varphi, \tag{20b}$$

where g(u) is partial amplification of the component of the array (in the function of the generalized coordinate u), averaged with respect to angle φ.

With regard to (20a) and (20b) and (15), instead of (17), we find the equality equivalent to it

$$\tau_q = \frac{1}{2kd}\int_{-kd}^{kd} g(u')e^{-iqu'}du'. \tag{21}$$

Using [2, 3], one can find an infinite set of equalities in notations (16) and (17)

$$\delta_{q0} = Q_q + \tau_q(q = 0, \pm 1, \pm 2, \ldots). \tag{22}$$

Multiplying each of relations (22) by $e^{iq\varphi}$ and adding them with respect to q in the range $-\infty$, $+\infty$, we find

$$1 = \tilde{Q}(\varphi) + \tilde{\tau}(\varphi), \tag{23}$$

where

$$\tilde{Q}(\varphi) = \sum_{q=-\infty}^{\infty} Q_q e^{iq\varphi}; \quad \tilde{\tau}(\varphi) = \sum_{q=-\infty}^{\infty} \tau_q e^{iq\varphi}. \tag{23a}$$

Based on (16), (21) and (23b), we find[1/]

[1/] The order of integration (with the substitution $u = q - p$, $q = p + u$) was changed during conversion of (20) and (21); the order of ... and ... changed upon conversion from (21) to (25a).

$$\tilde{Q}(\cdot) = |\tilde{S}(u)|^2, \tag{24}$$

$$I(\cdot) = \frac{\pi}{kd} \int \tilde{Q}(u)\,\delta_{\cdot}(\cdot - u)\,du$$

$$= \frac{\pi}{kd} \sum \tilde{Q}(\cdot - 2\pi n)\,\sigma\left(\frac{u}{kd}\right), \tag{25a}$$

where

$$\delta_{\cdot}(\xi) = \frac{1}{2\pi} \lim_{N \to \infty} \sum_{q=-N}^{N} e^{\cdot} \tag{25b}$$

is a periodic delta-function [5]:

$$\sigma(z) = \begin{cases} 0, & |z| > 1, \\ 1/2, & |z| = 1, \\ 1, & |z| < 1. \end{cases} \tag{25c}$$

Substituting (24) and (25a) into (23a) and returning to zero coordinates, we find

$$1 - |\tilde{S}(kd\cos\theta)|^2 = \frac{\lambda}{2d} \sum_{n} \left\{ \frac{1}{2\pi} \int_0^{2\pi} Q_0^{(S)}(\theta_n, \varphi)\,d\varphi\,\sigma(\cos\theta_n) \right\}, \tag{26a}$$

where summation (with fixed value of θ) is carried out by discrete angles determined by the equality

$$\cos\theta_n = \cos\theta + n\frac{\lambda}{d}, \tag{26b}$$

and the summation index is actually included in the range

$$-E\left[\frac{d}{\lambda}(1 - \cos\theta)\right] \le n \le E\left[\frac{d}{\lambda}(1 + \cos\theta)\right]. \tag{26c}$$

The function E(x) denotes the entire integer x.

For two-dimension periodic arrays, instead of (22) and (23a), we find

$$\delta_{\alpha}\delta_{\beta} \cdot Q_{\cdot} \cdot \delta_{\alpha\beta} \quad (\alpha, \beta = 0, \pm 1, \pm 2, \ldots), \tag{27}$$

$$|\ldots(Q(u, v) = \tilde{r}(u, v), \tag{28}$$

where $Q(u, v)$ and $\tilde{r}(u, v)$ are the corresponding two-dimensional Fourier series.

Transforming (18) similar to the linear case, we find

$$\tilde{Q}(u, v) = |\tilde{s}(u, v)|^2. \tag{29}$$

To find the function $\tilde{s}(u, v)$, we first transform expression (19), introducing the generalized coordinates:

$$u' = kd_1 \sin\vartheta \cos\varphi, \quad v' = kd_2 \sin\vartheta \sin\varphi. \tag{30a}$$

The element of the solid angle, according to (30a), is equal to

$$d\Omega = d\vartheta\, d\varphi = \frac{D(\vartheta, \varphi)}{D(u', v')} du'dv' = \frac{du'dv'}{kd_1 kd_2 \sqrt{1 - \left(\frac{u'}{kd_1}\right)^2 - \left(\frac{v'}{kd_2}\right)^2}}. \tag{30b}$$

With regard to the two-value nature of function $\vartheta(u', v')$, let us analyze expression (28) for the sum of integrals

$$\tau_{\alpha\beta} = \tau_{\alpha\beta}^{(+)} + \tau_{\alpha\beta}^{(-)},$$

where the upper (+) and lower (-) hemispheres, respectively, which are single-valued functions $\vartheta(u', v')$. Introducing the substitution $\vartheta = \pi - \vartheta'$ into $\tau_{\alpha\beta}^{(-)}$ and taking into account that $\sin\vartheta' = \sin\vartheta$, one can find the following expression for

$$\tau_{\alpha\beta} = \frac{1}{4\pi kd_1 kd_2} \iint_{(\sigma_R)} [s^{(+)}(u', v') + s^{(-)}(u', v')] \times \exp\{-i\alpha u' - i\beta v'\} \frac{du'dv'}{\cos\vartheta(u', v')}, \tag{31a}$$

$$s^{(+)}(u', v') = g_{\alpha\beta}^{(+)}[\vartheta(u', v'), \varphi(u', v')],$$
$$s^{(-)}(u', v') = g_{\alpha\beta}^{(-)}[\pi - \vartheta(u', v'), \varphi(u', v')], \tag{31b}$$
$$\vartheta(u', v') = \arcsin\sqrt{\left(\frac{u'}{kd_1}\right)^2 + \left(\frac{v'}{kd_2}\right)^2}, \quad \varphi = \frac{\pi}{2}.$$

$$\varphi(u', v') = \operatorname{Arctg}\frac{v' d_1}{u' d_2} \quad 2\pi. \qquad (31c)$$

[illegible] is applied to the area of the "radiation ellipse"

$$\left(\frac{u'}{kd_1}\right)^2 + \left(\frac{v'}{kd_2}\right)^2 \leqslant 1, \qquad (31d)$$

[illegible] the upper hemisphere onto the plane (u', v').

[illegible] similar to the linear case, we find

$$[illegible] \frac{\lambda^2}{4\pi A} \iint \frac{g(u', v')}{\cos\theta(u', v')} \delta_1(u - u') \delta_2(v - v') \, du' \, dv' = \frac{\lambda^2}{4\pi A} \sum_{n=-\infty}^{\infty} \sum_{p=-\infty}^{\infty} \frac{g(u - 2\pi n, v - 2\pi p)}{\cos\theta(u - 2\pi n, v - 2\pi p)} \, \sigma\left[1 - \left(\frac{u - 2\pi n}{kd_1}\right)^2 - \left(\frac{v - 2\pi p}{kd_2}\right)^2\right], \qquad (32a)$$

$$g(u, v) = g^{(+)}(u, v) + g^{(-)}(u, v), \qquad (32b)$$

[illegible] aperture area of the array per single component and σ[...] is [illegible].

[illegible], (31d) and (32a) and (32b), equality (2[illegible]) can be written in [illegible] form:

$$1 - |\tilde{s}(kd_1 \sin\theta\cos\varphi, kd_2 \sin\theta\sin\varphi)|^2 = \frac{\lambda^2}{4\pi A} \sum_{n} \sum_{p} [illegible] \qquad (3[illegible])$$

[illegible] values of θ, φ was carried over by discrete directions [illegible] by the relations

$$\sin\theta_{np}\cos\varphi_{np} = \sin\theta\cos\varphi - n\frac{\lambda}{d_1};$$
$$\sin\theta_{np}\sin\varphi_{np} = \sin\theta\sin\varphi - p\frac{\lambda}{d_2}. \qquad ([illegible])$$

and

$$0 \leqslant \theta_{\ldots} \ldots = 2,\ 0 \ldots q_{\ldots} \ldots 2\pi, \qquad \text{[illegible]} \tag{33c}$$

Relation (33a) coincides with that found in [1] at $d_1 = d_2$ and [illegible].

Let us note in concluding this section that the moving directions[1] in relations (26a) and (33a) should be excluded from consideration since the concept of partial radiation patterns is invalid for infinite arrays in these directions and one must use partial fields. Therefore, the value of $\varepsilon(1) = 1/2$ in formula (25c) has purely formal meaning determined by the apparatus of the Fourier series.

Some Theoretical Limitations of the Characteristics of Linear Arrays 10'

Relations (26a) and (33a) are equivalent to the law of conservation of energy for periodic systems of emitters and establish a close relationship between the scattering matrix of the system and the radiation patterns of the emitters. Hence, it specifically follows that one cannot be given the pattern of emitters independently of the scattering matrix when analyzing multicomponent arrays, especially if the period (or periods) of the array does not exceed the wavelength.

The indicated relations permit one to develop the series of principles of interest inherent to periodic emitting systems. These principles were first studied in [2] for two-dimensional arrays (at $d_1 = d_2$); some of them are considered below with respect to linear periodic arrays.

Since the right side of (26a) is the sum of nonnegative functions, [illegible] important inequalities follow from this relation[2]:

$$0 \leqslant \left|\tilde{S}(\ldots\cos\theta)\right| \leqslant 1; \tag{34}$$

---

[1] i.e., directions corresponding to [illegible] and [illegible] for linear arrays and [illegible] for two-dimensional arrays.

[2] We note that relation (34) was already found in [illegible] (true, with insufficient strictness).

$$0 < \sum_{n} g^{(e)}_{\varphi}(\theta_n) \cos\theta_n \leq \frac{2d}{\lambda};$$ (35a)

$$0 < g^{(e)}_{\varphi}(\theta) \leq \frac{2d}{\lambda},$$ (35b)

where

$$g^{(e)}_{\varphi}(\theta) = \frac{1}{2\pi}\int_{0}^{2\pi} g^{(e)}(\theta, \varphi)\, d\varphi$$ (35c)

is the partial amplification averaged with respect to φ.

The upper bound of amplification equal, according to (35b) to $2d/\lambda$, becomes physically obvious if one takes into account that maximum amplification does not exceed $2Nd/\lambda$ (N is the number of components) for a multicomponent axisymmetrical phased array with equal amplitude excitation of components and it is related to the amplification of the emitter by the known relation [2, 6]:

$$G_{\text{макс}} = N g^{(e)}(\theta_{\text{макс}}).$$ (36)

At $d < \lambda/2$ the sum in the right side of (26a) reduces to a single term and the scattering function in the range $-\pi \leq u \leq \pi$ satisfies the relations:

$$|\tilde{s}(u)|^2 = \begin{cases} 1 & \text{at } -\pi \leq u \leq -kd, \\ 1 - \frac{\lambda}{2d} g(\theta) & \text{at } -kd < u = kd\cos\theta < kd, \\ 1 & \text{at } kd < u \leq \pi. \end{cases}$$ (37) 105

from which it specifically follows that partial amplification (reverse amplification is invalid!) quite specifically averaged with respect to φ corresponds to a specific scattering matrix at $d < \lambda/2$.

It is interesting to note in this regard that due to the evenness of [illegible] (see [11]), function $|\tilde{s}(u)|^2$, according to (37), is symmetrical with respect to

the plane perpendicular to the axis of the array. In this case the pattern of the emitter taken separately from the system can also be asymmetrical.

It also follows from (37) that the efficiency of a linear phased array [see (4)] with period in the range of a half-wave is equal to zero at $kd = |\gamma| = \pi$; this phenomenon is physically obvious since the array under consideration has no main beams in the range of effective angles with this phasing.[1]

Based on formulas (4), (35b) and (37), it is easy to find the following inequality:

$$\eta_{\text{ef}}^{(e)} \leq \frac{2d}{\lambda} < 1. \tag{38}$$

It follows from (38) that first, the efficiency of the emitter of the array under consideration (with waveload of the feeder lines of the remaining components) does not exceed $2d/\lambda$ and second at least one component of the scattering matrix of the system is distinct from zero.

A somewhat more specific discussion of the components of matrix [s] can be found on the basis of relations (37).

For example, one can show that emitters can be uncoupled ($s_{-2} = s_{-1} = s_{+1} = s_{+2} = \ldots = 0$) only in the trivial case--at $|s_0| = 1$, i.e., when they do not emit. Actually, (37) is identically satisfied at $|\tilde{s}(u)| = |s| = 1$ and $F_1^{(e)}(\theta, \varphi) = 0$, and at $|s|<1$ and $s_n = 0 (n \neq 0)$, based on (4), (35) and (37), we find the inequality

$$D_{\text{ef}}^{(e)}(\theta) \leq \frac{2d}{\lambda} \cdot \frac{1 - |\tilde{s}(kd\cos\theta)|^2}{\eta^{(e)}} \leq \frac{2d}{\lambda} < 1, \tag{39}$$

which is obviously contradictory to the definition of the front-to-rear ratio.

[1] The term efficiency is the ratio of the finicky of the array to the sum of losses in the emitters and in the surrounding space. In a planar array of finite dimensions in the case of beam divergence, only its external component is practically efficiency is on the order of 3/4.

We note that inequality (39) does not at all prohibit achievement of 100-percent efficiency when an array is operating in the scanning mode (i.e., with linear-phase excitation of its components). According to (6) and (34), a return of function $\tilde{S}(u)$ to zero at $-kd < u < kd$ is required for this, i.e., in the interval of effective angles. It follows from (37) that the scattering function of the indicated "ideal" phased array satisfies the condition:

$$|\tilde{s}_{\text{ид}}(u)| = \begin{cases} 0 \text{ at } & -kd < u < kd, \\ 1 \text{ at } & kd < |u| < \pi, \end{cases} \tag{40}$$

while partial amplification is

$$s_{\text{ид}}^{(c)}(u) = \frac{2d}{\lambda} = \text{const}, \tag{41}$$

i.e., its radiators are omnidirectional.[1/] The efficiency of the component of an ideal array, as follows from (41), reaches its upper bound equal to $2d/\lambda$. The components of matrix $[s_{\text{ид}}]$, according to (40), are expressed in the form

$$s_{\text{ид}\,n} = \frac{1}{\pi} \int_{kd}^{\pi} e^{i\varphi(u)} \cos nu\,du \quad (n = 0, \pm 1, \pm 2, \ldots), \tag{42}$$

where $\varphi(u)$ is some real function.

It is clear with regard to the given remark that matching of a phased array for which $|s(\theta)| \equiv 1$ is necessary and matching its components in the generally accepted meaning ($|s_0| \ll 1$) are completely different concepts. In a number of cases, for example, with components located close to each other ($d \ll \lambda$), matching the entirety may even lead to mismatching of the phased array and on the other hand, wide-angle matching of the latter may correspond to appreciably unequal components.

[1/] Omnidirectionality, which can be known as formerly with finite current flow, is here the result of the infinity of the scanning considered in the absence of losses in the radiators and the mutual influence etc.

With [illegible] to arrays with period $d > \lambda/2$, many of the restrictions noted above for them are no longer valid. Specifically, it essentially becomes permissible that $s_0 = s_{\pm 1} = s_{\pm 2} = \ldots = 0$ and $\eta^{(c)} = \eta(\phi) = 1$. Mutually single-valued coincidence of type of (37) between the amplification of the emitter and the modulus of the scattering function of the system is retained at $d < \lambda$ in the range $-(2\pi - kd) < u < 2\pi - kd$, corresponding only to part of the sector of effective angles ($\pm$arc sin $\left(\frac{\lambda}{d} - 1\right)$ from the normal to the aperture).[1]

Conclusions

1. Expressions were found for the efficiency and power efficiency factor for linear and two-dimensional periodic arrays with excitation of them by voltage generators having identical internal impedances and arbitrary emf.

2. The relationship between the scattering matrix and amplification of the emitter was established in a linear periodic array. This relationship was found for a two-dimensional array at more general assumptions than in [2] and namely when the periods of the array are arbitrary and the radiation of energy is not limited by a half-space.

3. A number of theoretical restrictions was found on the basis of the relationship between the scattering matrix and the amplification of the emitter of a linear periodic array for its characteristics, specifically:

a) the amplification of the emitter of a linear array averaged with respect to ϕ (with envelope of the feeder lines of all components) does not exceed $2d/\lambda$;

[1] However, as follows from (36a), only one function [illegible] corresponds to the specific function [illegible] at any values of d. [illegible] relation [illegible] and [illegible])) is valid only at $d < \lambda/2$.

b) at $d < \lambda$ the amplification indicated in paragraph a is a function [illegible] with respect to a plane perpendicular to the axis in the range of [illegible];

[illegible] coupling is inevitable between emitters of an array with period

[illegible] resistance of an emitter (with wave load of feeder lines of the [illegible] does not exceed $2\sigma/\lambda$ at $d < \lambda/2$.

[illegible] emitters of an array can essentially be uncoupled and matched and [illegible] with 100 percent with a period exceeding $\lambda/2$.

References

[illegible]